Ph.D. degree in Systems Medicine (curriculum in Molecular Oncology)

European School of Molecular Medicine (SEMM)

University of Milan and University of Naples "Federico II"

Settore disciplinare: MED/04

Structural and functional consequences of p63 mutations causative of AEC syndrome

Claudia Russo

Ceinge, Naples

Matricola n. R11123

Supervisor: **Prof. Caterina Missero**
Ceinge, Naples

Internal Supervisor: **Prof. Tommaso Russo**
Ceinge, Naples

External Supervisor: **Prof. Gian Paolo Dotto**

Academic Year 2017-2018

TABLE OF CONTENTS

LIST OF ABBREVIATIONS

AEC syndrome Ankyloblepharon- Ectodermal defects- Cleft lip/palate syndrome

EEC syndrome Ectrodactyly, Ectodermal defects-Cleft lip/palate syndrome

SHFM Split-hand/foot malformation

+/L K14-Cre;$p63^{+/floxL514F}$

L/L K14-Cre;$p63^{floxL514F/floxL514F}$

het $p63^{+/floxL514F}$

hom $p63^{floxL514F/floxL514F}$

APRs aggregation propensity regions

Dsc3 Desmocollin 3

Krt14 Keratin 14

Krt5 Keratin 5

Krt8 Keratin 8

UPR Unfolded Protein Response

FIGURES INDEX

ABSTRACT

p63, a p53 family member, is a tetrameric transcription factor required for the development and differentiation of stratified epithelia. Heterozygous mutations in p63 are causative of a group of autosomal dominant human disorders characterized by ectodermal dysplasia, orofacial clefting and limb malformations. More specifically, mutations clustering in the C-terminal domain of p63 cause Ankyloblepharon-Ectodermal defects-Cleft lip/palate (AEC) syndrome, a life-threatening disorder characterized by severe extended skin erosions.

Here we show that multiple AEC-associated p63 mutations lead to protein misfolding and aggregation, as observed also in human keratinocytes isolated from an AEC patient and in mouse keratinocytes obtained from a conditional knock-in mouse model for AEC syndrome, recently generated in our laboratory, that phenocopies the skin clinical features found in human patients. In AEC mice the aggregated p63 mutant protein causes an impaired expression of endogenous p63 target genes, among which are keratins and desmosomal proteins involved in cell adhesion and in mechanical resistance, leading to severe skin fragility and erosions. Importantly, we found that abolishing the aggregation of p63, by introducing mutations that drastically reduce the aggregation propensity of AEC mutants, allowed to rescue p63 transcriptional functions, thus suggesting that impaired p63 transactivation activity is uniquely associated in AEC syndrome with exposure of aggregation-prone sequences. In addition, our studies focused on the therapeutic potential of these findings and suggested possible approaches to treat the AEC syndrome based on targeting and strengthening the endogenous protein disaggregation machinery or using drugs designed to chemically assist the correct folding of the mutant protein.

1. INTRODUCTION

1.1 The epidermal barrier: structure and functions

The epidermis is a highly specialized epithelium involved in several fundamental protective functions: it prevents dehydration regulating the loss of water and solutes, participates in thermoregulation and, being the outermost compartment of the skin, it acts as physical barrier against mechanical trauma, ultraviolet radiations, chemical agents and microorganisms. The epidermal barrier is composed by multiple layers of keratinocytes, cells that undergo a series of morphological and physiological changes during epidermal maturation, giving rise to the complex architecture of the tissue. Four layers can be distinguished in the skin, from outside to inside: the cornified layer (*stratum corneum*), the granular layer (*stratum granulosum*), the spinous layer (*stratum spinosum*) and the basal layer (*stratum basale*), which is attached to the underlying basement membrane through a series of adhesion molecules such as hemidesmosome, integrins, laminin and anchoring fibrils (Fig. 1). The basement membrane forms a boundary of extracellular matrix between the epidermis and the underlying dermis.

The stratified squamous epithelium of the epidermis is maintained by cell division within the basal layer. Here, epidermal stem cells ensure the self-renewal of the tissue giving rise to daughter stem cells and to transit amplifying cells, which display a more limited proliferative capacity and represent the major cells type in the basal layer of the developing and mature epidermis. After few doublings, some transit amplifying cells, generated by asymmetric mitoses, undergo a cell cycle arrest and initiate a terminal differentiation program. They first migrate outward in the spinous layer, where keratinocytes grow larger, establish robust intercellular connections (Simpson et al.,2011) and switch expression of basal layer specific

keratins, such as keratin 5 and keratin 14, to keratin 1 and keratin 10, typical of spinous layer (Fuchs and Green, 1980). Then, spinous keratinocytes differentiate to form the granular layer, where cells are characterized by the presence of numerous electron dense keratohyalin granules packed with the protein profilaggrin in their cytoplasm. Cells in the granular layer flatten, assemble a water-impermeable cornified envelope underlying the plasma membrane and express filaggrin (FLG) and loricrin (LOR), typical markers of the granular layer. Then, cornified envelope proteins, which are rich in glutamine and lysine residues, are synthesized and deposited under the plasma membrane of the granular cells. Cross-linking of structural proteins and lipids leads to the assembly of the highly cornified outermost layer of the epidermis, the *stratum corneum*. Finally, keratinocytes from the *stratum corneum* release lysosomal enzymes to degrade major organelles, including the nucleus. The dead stratum corneum cells create an impenetrable layer that is continually replaced (Fuchs, 2007). This continual stratification and differentiation of keratinocytes allows the epidermis maintenance and requires the coordinated and sequential regulation of several genes. Among these, the transcription factor p63 plays a crucial role in the early stages of skin development (Koster et al., 2004), being abundantly expressed in the basal layer of the epidermis.

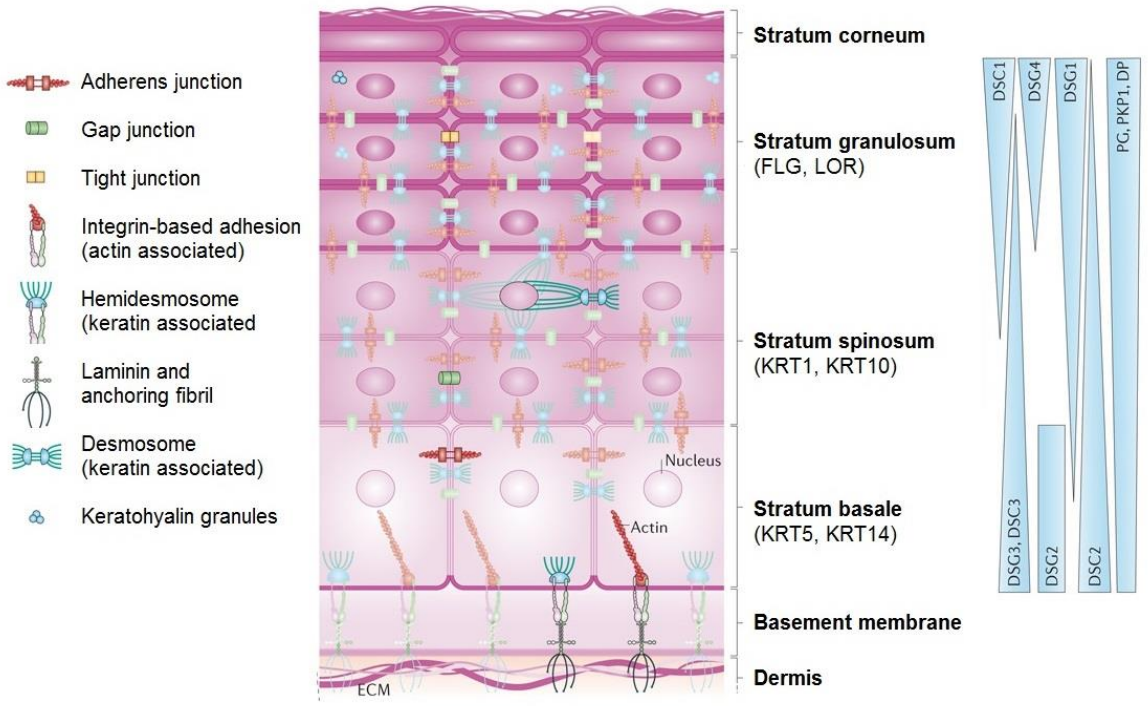

Figure 1. The epidermis. The epidermis is a stratified squamous epithelium composed by four layers resting on the basement membrane, which separates the epidermis from the underlying dermis. During epidermal maturation keratinocytes undergo a terminal differentiation driven by a gradual and sequential expression of specific cytoskeletal and junction proteins, which underlies the tissue morphogenesis. Desmogleins (DSG1, DSG2, DSG3, DSG4) and desmocollins (DSC1, DSC2, DSC3) are desmosomal cadherins that bind to plakoglobin (PG) and plakophilin (PKP) for the assembly of the desmosomes. Desmoplakin (DP) anchors keratin intermediate filaments to desmosomal plaques. (adapted from Simpson et al., 2011).

1.2 The transcription factor p63, a master regulator of epidermal development

TP63 gene encodes a tetrameric transcription factor that plays an essential role in the commitment of simple ectoderm to epidermal lineages and is required for the development of stratified epithelia (Koster et al., 2004; Nguyen et al., 2006; Truong et al., 2006). p63 belongs to the p53 family, consisting of three genes encoding the transcription factors p53, p63 and p73. The p53 family members share an highly homologous DNA binding domain (DBD), therefore, p63 binds to canonical p53 DNA-binding sites and shares some biological functions with the other members of the family (Vanbokhoven et al., 2011; Yang et al., 1998).

TP63 gene consists of 16 exons located on chromosome 3q28. Two classes of p63 proteins are generated by two alternative promoters, TAp63 and ΔNp63, and each of them includes three distinct variants, α, β, and γ isoforms, resulting from alternative splicing events at 3' end (Fig. 2). More specifically, TAp63 proteins contain an N-terminal transactivation domain which shares 25% of identity with N-terminal region of full-length p53 (Yang et al., 2002). TAp63 is expressed at very low levels in most tissues, whereas it is constitutively expressed in female germ cells in a dimeric inactive conformation during meiotic arrest (Suh et al., 2006; Crum et al., 2010). Upon DNA damage TAp63 dimers turn into active tetramers leading to oocytes death (Deutsch et al., 2011). Otherwise, ΔNp63 lacks of the typical N-terminal transactivation domain, but it retains two cryptic transactivation domains: the region including the first 26 N-terminal amino acids and a PPxY motif corresponding to exon 11/12 (Helton et al., 2006). ΔNp63 is found in a tetrameric form and the α isoform is the most abundantly expressed in the basal layer of the epidermis and in other stratified epithelia, where it plays an essential role in keratinocyte proliferation (Truong et al., 2006; Senoo et al., 2007; Antonini et al.,

2010), stratification (Koster and Roop, 2004; Truong et al., 2006) and cell adhesion (Carroll et al., 2006; Koster et al., 2007; Ferone et al., 2013), but it suppresses terminal differentiation, being involved in coordinating a complex balance between keratinocyte self-renewal and differentiation (Nguyen et al., 2006). Importantly, ΔNp63 is a transactivator for most epidermal target genes, but it can also act as a repressor for some genes (Antonini et al., 2010; De Rosa et al., 2009; Ramsey et al., 2011). ΔNp63α has a crucial role also in embryonic development of stratified epithelia, as it is specifically expressed in the surface ectoderm at E7.5-E8, prior to Krt5 and Krt14 expression, and it continues to be expressed during skin development and in the basal proliferative layer in postnatal life (Laurikkala et al., 2006). The α isoform is the longest one and contains a sterile-α-motif (SAM) domain, encoded by exons 13 and 14 in the p63a gene, and a post-SAM (PS) domain, encoded by exon 14 and located downstream the SAM domain. The SAM domain is a putative protein interaction module present in a wide variety of proteins, whose function is still unknown. This domain commonly interacts with similar SAM domains by homo- and hetero-oligomerization (Stapleton et al., 1999; Thanoset al., 1999), but it can also mediate intermolecular association with nucleic acids, lipids or other proteins not containing SAM domain (Schultz et al., 1997; Serra-Pages et al., 1995). The PS domain is about the same length as the SAM domain and can be divided in two subdomains. The N-terminal subdomain (45 amino acids) contains a transcriptional inhibitory (TI) sequence that forms a closed inactive dimer with the TA domain (Coutandin et al., 2016; Straub et al., 2010). The C-terminal subdomain (25 amino acids) contains a sumoylation site involved in regulating p63 concentrations (Straub et al., 2010).

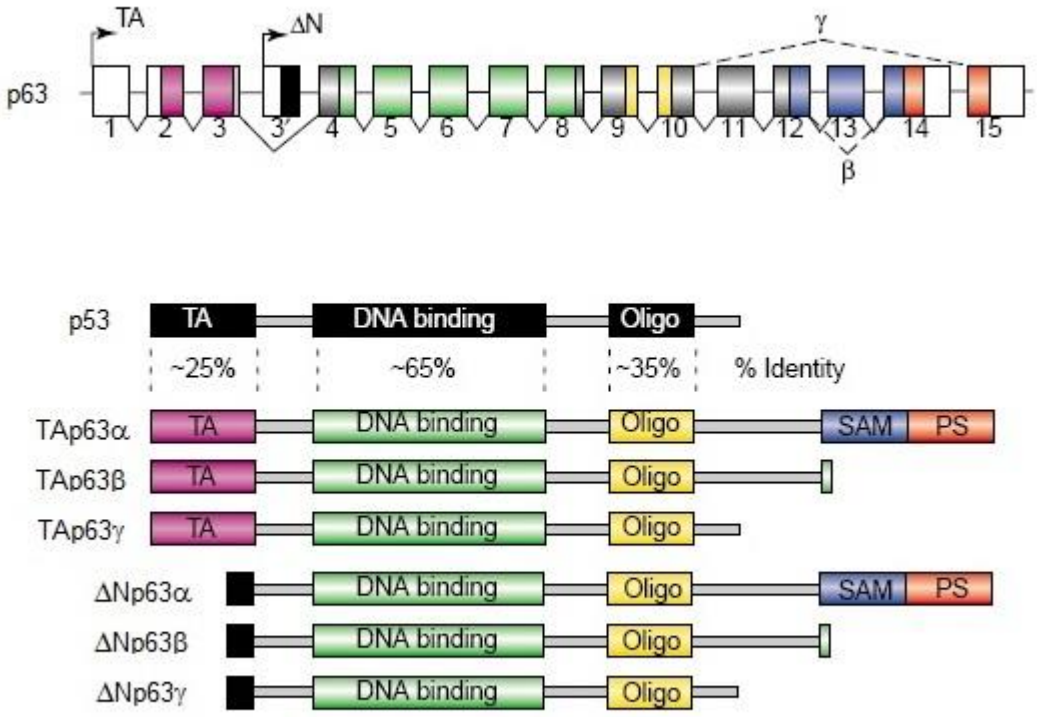

Figure 2. p63 gene and its isoforms. Schematic representation of p63 gene structure and isoforms. Two alternative promoters give rise to TAp63 or DNp63 transcripts, whereas at the 3' end alternative splicing events generate α, β or γ isoforms. In the lower panel, protein domains conserved in p53 family are shown: Transactivation domain (TA), DNA binding domain, Oligomerization domain. SAM and PS domains in p63 α isoforms are absent in p53 full-length gene. The percentage of identity between p53 and p63 conserved domains are indicated (adapted from Yang et al., 2002).

1.3 The C-terminus of p63α isoform

As p53 family members, p63 and p73 possess a domain structure similar to p53 but can contain variable C-terminal extensions, resulting by alternative splicing events. More specifically, the full-length α isoform of p63 and p73 is characterized by a sterile α-motif (SAM) domain at the C-terminus followed by a post-SAM (PS) domain, both not present in human p53. Furthermore, differently from p63β and p63γ isoforms, that display p53-like functions, p63α has little or no p53-like activity, suggesting that these C-terminal extensions could be responsible for functional differences between p63 and p53 (Thanos and Bowie, 1999).

The **SAM domain** is composed by ~70 amino acids and consists of protein-protein interaction modules found in a series of proteins involved in the regulation of developmental processes, signal transduction and transcription (Schultz et al., 1997). Although SAM domains adopt similar folds, they are remarkably versatile in their binding properties. Some identical SAM domains can interact with each other to form homodimers or polymers. In other cases, SAM domains can bind to other related SAM domains, to non-SAM domain-containing proteins and even to RNA (Qiao et al., 2005).

The solution structure of the C-terminal domain of human p63 (505-579) was solved through NMR spectroscopy. The resulting structure shows the characteristic five helix bundle topology observed in other SAM domains (Schultz et al., 1997). It includes helix 1 (α1; residues 514–521), helix 2 (α2; residues 527–533), a short 310 helix (H3; residues 538–542), helix 4 (α4; residues 546–551), and helix 5 (α5; residues 556–573). The five helices are tightly packed together via an extended hydrophobic core and form a globular and compact structure. The N-terminal (residues 505–508) and the C-terminal (residues 576–579) regions are found to be highly mobile in solution (Cicero et al., 2006).

Missense mutations in the SAM domain of p63 cause Ankyloblepharon Ectodermal defects Cleft lip/palate syndrome (AEC, OMIM 106260) and Rapp Hodgkin syndrome (RHS, OMIM 129400) (McGrafth et al., 2001; Kantaputra et al., 2003), very similar to AEC one, that will be discussed later. The high resolution crystal structure of the p63α SAM domain was determined to investigate the effect of several AEC-associated mutations on the stability of the domain. The aliphatic isoleucine and leucine residues (I549, L553, L556, I573, I576, L584, L587, I589, I597 and I601), that are part of the compact hydrophobic core, are highly conserved in all SAM domains (Fig. 3a). Compared with the wild-type, AEC-associated mutations L553F, C561G, C561W, G569V, Q575 and I576T are all significantly destabilizing, probably because of the structural features of the wild-type protein (Fig. 3b). Mutation L553F, which is close to F552, would probably cause a severe steric clash between the two phenylalanine rings and result in overcrowding in the hydrophobic core (Sathyamurthy et al., 2011). However, for two AEC-associated SAM mutations, G534V and T537P, the main effect does not concern a structural disruption but instead a perturbation of the dynamical properties. Molecular dynamics (MD) simulation reveals that the two mutants acquire a degree of helical content higher than that of the wild type protein, excluding a structural collapse. In contrast, both mutants display a similar increase in flexibility in helix 4 and at the N-terminal region, suggesting that the pathological behavior of p63 observed in the presence of these mutations could be associated with the occurrence of new recognition properties induced by a varied flexibility (Cicero et al., 2006).

a b

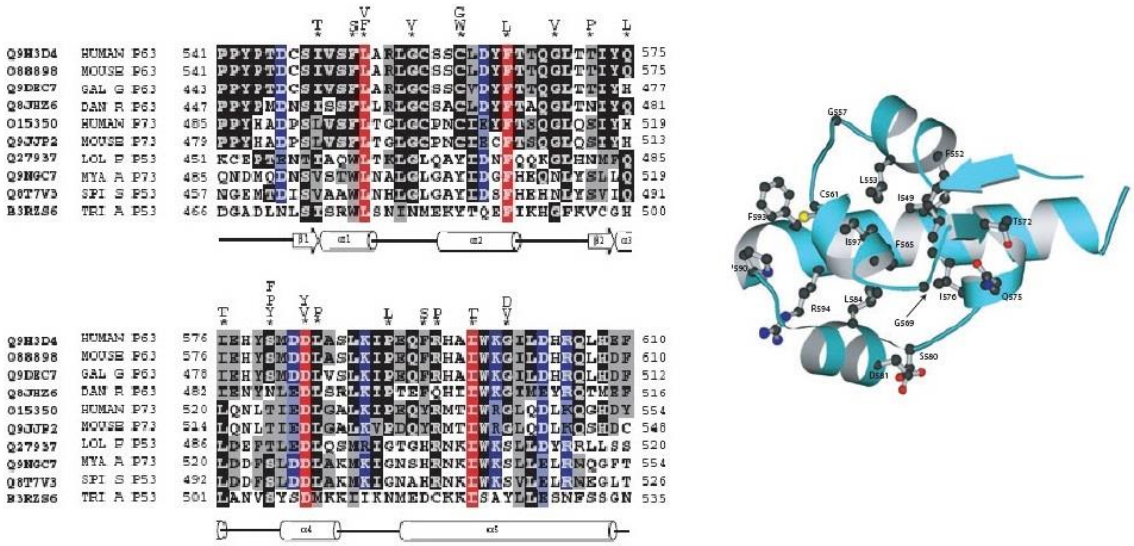

Figure 3. SAM domain of p63α. a) CLUSTALW sequence alignment of SAM domains of p53 family members. Conserved residues are shown in red. Conserved and partially conserved hydrophobic residues are shown in black and grey, respectively. Conserved and partially conserved charged residues are shown in blue and light blue, respectively. The positions and type of AEC mutations are shown above the sequence alignment. A diagrammatic representation of the five helices is shown below the alignment. b) Ribbon representation of the p63α SAM domain showing the position of mutations that are associated with AEC syndrome. (adapted from Sathyamurthy et al., 2011).

The **PS domain** is located after the SAM domain and contains two individual components: one that uses an intramolecular interaction mechanism to mask and inhibit the transactivation domain and another that is involved in sumoylation. More specifically, the N-terminal subdomain consists of 45 amino acids and is called also “Trans-Inhibitory Domain” (TID), as it binds the TA domain of p63 forming a close inactive conformation and blocking its transactivation function. This inhibitory mechanism is crucial in regulating quality control in oocytes, where TAp63α is kept

in an inactive dimeric state and switches to the tetrameric active conformation upon DNA damage, inducing cell death (Deutsch et al., 2011).

The intramolecular interaction mediated by the TID domain does not involve ΔNp63α isoform, as it lacks of its own TA domain. However, since p63 tetramerizes and can also form hetero-oligomers between different p63 isoforms, the TID domain of ΔNp63α can interact with the TA domain of another protein within the tetramer, acting in a dominant-negative manner (Serber et al., 2002).

The C-terminal portion of PS domain, composed by the last 25 amino acids, contains a sumoylation site IKEE (K637), targeted by SUMO-1 (Small Ubiquitin-like Modifier 1) for proteasome mediated degradation (Fig. 4). Some mutations falling within the SAM and post-SAM domains of p63α can alter the sumoylation capacity and lead to a strong increase of the transcriptional activities of p63, suggesting that sumoylation has a negative effect on p63 transactivation function. The findings that ΔNp63α protein levels are regulated by SUMO-1 and that this regulation is altered when the PS domain is mutated suggest that SUMO conjugation to p63 plays a critical role in regulating the biological activity of p63, by controlling its intracellular concentrations (Ghioni et al., 2005; Straub et al., 2010).

NMR studies of the PS domain has shown that this domain lacks of a secondary structure. Interestingly, the TID domains of p63 and p73 display a low intrinsic aggregation propensity which confers self-aggregation ability to the wild-type proteins also in the tetrameric form, as they remain readily accessible (Kehrloesser et al., 2016).

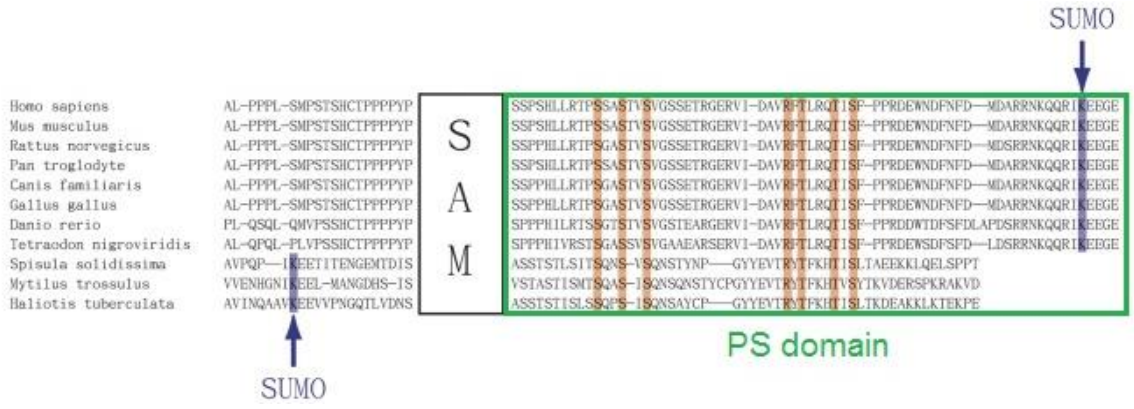

Figure 4. PS domain of p63α. CLUSTALW sequence alignment of PS domains of various vertebrate and invertebrate species. Strictly conserved amino acids are labeled in red. The conserved IKEE sumoylation motif is labeled in blue. In invertebrate species the sumoylation sequence is located upstream of the SAM domain. (adapted from Straub et al., 2010).

1.4 p63-associated disorders

Heterozygous mutations in TP63 gene cause a group of autosomal dominant human syndromes characterized by various combinations of ectodermal dysplasia, orofacial clefting and limb malformations (Rinne et al., 2006). p63 transcription factor plays in fact an essential regulatory role in several developmental processes during embryogenesis, being required for the differentiation of ectodermal derivatives such as hair, nails, mammary glands, teeth (Mills et al., 1999). Furthermore, it transcriptionally activates *Fgfr2 gene* to sustain epithelial and mesenchymal proliferation during palatal growth (Ferone et al., 2012), *Irf6 gene* to regulate palatal fusion (Thomason et al., 2010), cell adhesion molecules Dsp, Dsc3, Dsg1 (Ferone et al., 2013), Pvrl1 and Pvrl4 (Mollo et al., 2015) to control epidermal cell junctions and, importantly, it maintains the apical ectodermal ridge, a stratified epithelium essential for limb development (Yang et al., 1999).

Accordingly, mice lacking the p63 gene(p63-/-) die soon after birth with severe defects of skin and all stratified epithelia and their derivatives, craniofacial abnormalities and impaired limb formation (Mills et al., 1999; Yang et al., 1999; Vanbokhoven et al., 2011).

At least five different syndromes caused by mutation in p63 have been described: Ectrodactyly, Ectodermal defects-Cleft lip/palate syndrome (EEC, OMIM 604292), Ankyloblepharon-Ectodermal defects-Cleft lip/palate syndrome (AEC, OMIM 106260), Limb Mammary Syndrome (LMS, OMIM 603543), Acro-Dermato- Ungual-Lacrimal-Tooth syndrome (ADULT, OMIM 103285) and Rapp-Hodgkin Syndrome (RHS, OMIM 129400). Furthermore, some p63 mutations can cause non-syndromic single malformations, such as Split Hand/Foot Malformation (SHFM4, OMIM 605289) (Ianakiev et al., 2000) and isolated cleft lip (NSCL) (Rinne et al., 2007).

P63 mutations are generally clustered in specific domains for each syndrome or occur in the same domain but display distinct characteristics (Fig. 5), suggesting a genotype-to-phenotype correlation. Anyway, p63 syndromes share at least one of the three main phenotypic hallmarks of p63 syndrome family (Fig. 6): ectodermal displasia, orofacial clefting, limb defects (Rinne et al., 2006).

EEC represents a prototype of p63 syndromes as it combines all the phenotypical features described above and is mainly caused by point mutation in the DNA binding domain (DBD) of the p63 gene (Fig. 5) that most likely impairs the DNA-binding properties of the transcription factor (Celli et al., 1999).

EEC phenotype includes abnormal development of ectodermal structures such as teeth, skin, hair, nails and sweat glands, orofacial clefting and limb malformations, more specifically ectrodactyly and syndactyly (Rinne et al., 2007).

LMS was the first p63 syndrome linked to chromosome region 3q27. Mutations causative of LMS are located in the N- and C-terminus of the p63 gene.

LMS phenotype is mainly characterized by malformations of the hands and/or feet, similar as in EEC, and hypoplastic nipples and mammary glands. Lacrimal duct obstruction, dystrophic nails, hypohydrosis and teeth defects are observed, although ectodermal defects are much less prominent than in EEC syndrome. Hair and skin defects are rarely detected whereas orofacial clefting, always in form of cleft palate, is present in 30% of LMS patients (van Bokhoven and Brunner, 2002).

ADULT syndrome phenotype is overall overlapping to LMS one, except for the absence of orofacial clefting and the presence of hair and skin defects. In some ADULT patients, a point mutation in exon 8, changing R298 in the DNA binding domain into either a glutamine or a glycine, has been found. Differently from EEC syndrome hot-spot mutations, R298 is not located close to the DNA-binding interface, thus mutation of this arginine does not affect DNA binding (Duijf et al., 2002). Two other mutations are located in the N-terminus.

RHS share most features with **AEC**, but is differentially classified because of the lack of skin erosions and the absence of ankyloblepharon in Rapp-Hodgkin syndrome. In both syndromes clefting in lip and/or palate is equally frequent whereas limb malformations are absent. AEC and RHS mutations are located in the same region of the p63 protein, the C-terminus, and are either point mutations in the SAM domain or deletions in the SAM or PS domains (Celli et al., 1999; McGrath et al., 2001; Barrow et al., 2002; van Bokhoven and Brunner, 2002; Kantaputra et al., 2003). The strong overlap between AEC and RHS, in terms of localization of hot spot mutations and phenotype, suggests that they could be variable manifestations of the same clinical entity (Bertola et al., 2004; Rinne et al., 2007).

SHFM is non-syndromic disorder associated to several chromosomal loci in the human genome. About 10% of SHFM patients have a p63 mutation (Rinne et al., 2006) and it is used to refer to their condition as SHFM4 (Ianakiev et al.,2000).

SHFM4 is a pure limb malformation (ectrodactyly and syndactyly) condition, without orofacial clefting or ectodermal dysplasia. Several mutations dispersed along the p63 gene are causative of SHFM4, among which splice-site mutation (3'ss intron 4), missense mutations (R58C, K193E, K194E, R280C/H) and stop-mutations (Q634X, E639X) (Ianakiev et al., 2000; van Bokhoven et al., 2001; Zenteno et al., 2005). Possibly, SHFM is caused by altered protein degradation, even though different degradation routes are involved (Rinne et al., 2007).

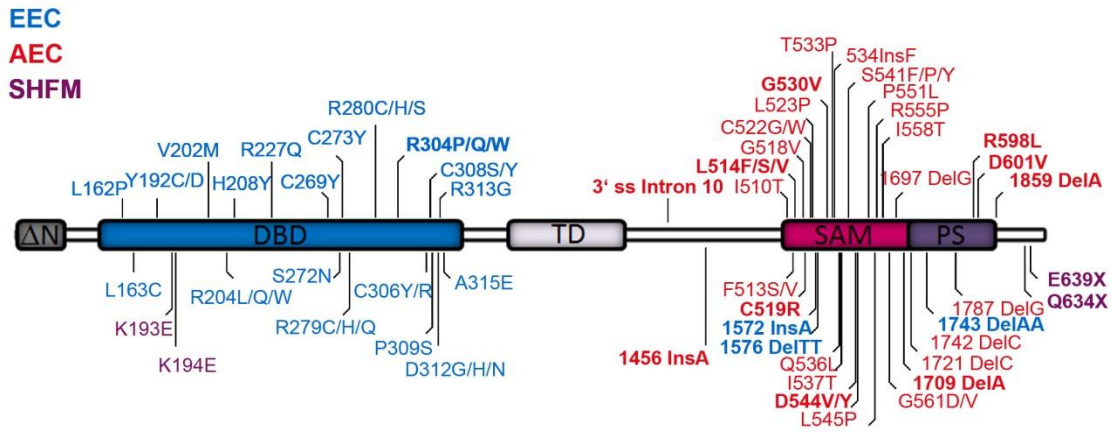

Figure 5. p63 disease-causative mutations. Spectrum of some p63 mutations causative of the indicated disorders, color-coded for each disease (other p63 syndromes are not represented). EEC-associated mutations affect mainly the DNA binding domain whereas AEC-associated mutations are clustered in SAM and TI domains (adapted from Russo et al., 2018).

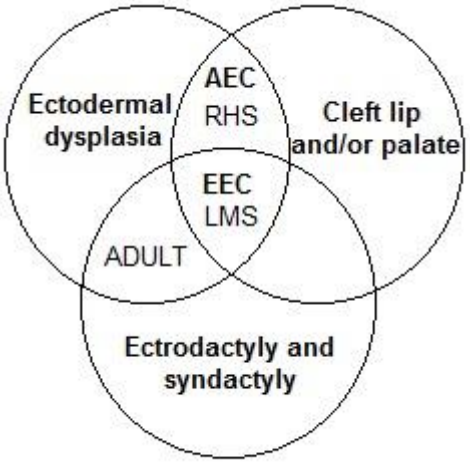

Figure 6. The three hallmarks of p63 syndrome family. Scheme of overlapping phenotypes found in p63 syndromes. EEC and LMS combines all the three phenotypical features, although in LMS ectodermal defects are less severe. AEC and RHS are mainly characterized by ectodermal dysplasia and orofacial clefting, whereas ADULT expresses ectodermal and limb defects (adapted from Brunner et al., 2002).

1.5 The AEC syndrome

Among the p63 syndromes, the Ankyloblepharon-Ectodermal defects-Cleft lip/palate (AEC) syndrome, also known as Hey-Wells syndrome, is characterized by the most severe skin symptoms, including congenital erythroderma, skin fragility, blistering and extensive erosions, often accompanied by crusting and secondary infection (Hay and Wells 1976; McGrath et al. 2001; Julapalli et al., 2009). Widespread skin erosions typically appear at or soon after birth, involving the scalp, head and neck, skin folds, palms and/or soles leaving, in some cases, up to 70% denuded skin. By 4 – 5 years age erosions could disappear, except for the head and auricular region (Rinne et al., 2006). The symptoms affecting adult patients are palmoplantar hyperkeratosis and erosive palmoplantar keratoderma, that can lead to bleeding after long walks.

Although skin lesions are the distinctive signs of AEC syndrome, other features are also found such as congenital fusion of the eyelids (ankyloblepharon), ectodermal dysplasia with severe involvement of the skin and its derivatives (teeth, nails, mammary glands) and cleft palate with or without cleft lip, occurring with different penetrance (Fig. 7).

More specifically, clefting occurs approximately in 80% of AEC patients, whereas ankyloblepharon occurs only in 44% of AEC cases. Hearing loss has been reported in about 40% of the patients. AEC patients have nail and teeth defects in about 75–80% of cases (Rinne et al., 2006).

AEC syndrome mutations are mainly clustered in the C-terminal portion of p63 (Fig. 5), either as missense mutations in the SAM domain and more rarely in the TI domain or as frame-shift mutations in the TI domain, that lead to an abnormal elongation of the protein (Rinne et al., 2009). The specific clustering of p63 mutations and the uniqueness of the skin phenotype in AEC syndrome suggest a genotype-to-phenotype correlation, although little is known about the biological and molecular mechanisms underlying the skin erosions, that could be life-threatening in some cases, leading to aggravated lesions with bleeding and infections. To date, treatment is limited to wound care and prevention of infections by antibiotic administration.

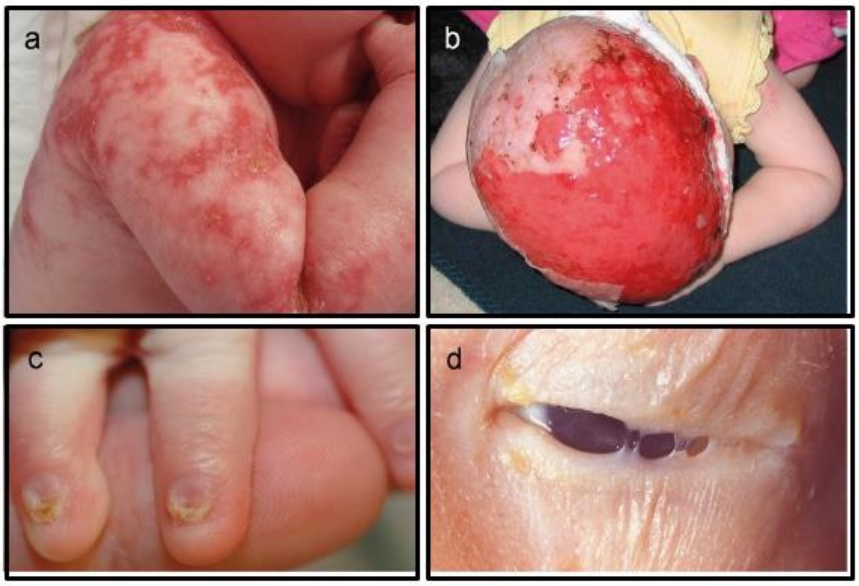

Figure 7. Clinical signs in AEC infants. a) AEC patient with a close up of reticulated scarring resulting from skin erosions healing processes. b) Scalp erosions hemorrhagic crusting, granulation tissue and secondary infection. c) Dystrophic fingernails of AEC patients, characterized by small nails with partial loss/absence and distal fraying of the nail plate. d) Focal fusion of the eyelids (ankyloblepharon) (adapted from Ferone et al., 2015).

1.6 AEC mouse model

To characterize the functional and molecular alterations correlated to p63 mutation in AEC syndrome, a first constitutive knock-in mouse model ($p63^{+/L514F}$) was previously generated in our laboratory (Ferone et al., 2012). This model carries a leucine to phenylalanine substitution in position 514 (L514F) of the p63 protein and closely phenocopies the clinical hallmarks of the human disorder (Ferone et al., 2012, Ferone et al., 2013) (Fig.8). The L514 amino acid was chosen as a representative AEC mutation site as it localizes in the first helix of the SAM domain, where it seems to be a critical site for p63 protein stability. Indeed,

L514 is found mutated in three different amino acids (phenylalanine, valine or serine) in AEC patients, so any mutation in this region is likely to affect the overall structure and stability of the protein by altering the packing of the helices. Moreover, the substitution of a leucine with a phenylalanine probably causes a severe steric clash with another close phenylalanine ring in the folded protein (McGrath et al., 2001; Rinne et al., 2007).

Similar to AEC patients, $p63^{+/L514F}$ mice display hypoplastic and fragile skin, ectodermal dysplasia and cleft palate, associated with a reduced epithelial cell proliferation during development (Ferone et al., 2012). This phenotype is largely overlapped to that of $Fgfr2b^{-/-}$ mice, in which the impaired FGF signaling leads to defects of epithelial cell proliferation during embryonic development (Petiot et al, 2003; Rice et al, 2004). In agreement, Fgfr2b and Fgfr3b expression is downregulated in $p63^{+/L514F}$ mice, suggesting that impaired FGF signaling downstream of p63 is likely an important determinant of reduced ectodermal cell proliferation and defective epidermal self-renewing compartment in AEC syndrome (Ferone et al., 2012). Importantly, skin fragility, a typical feature of AEC patients, is found also in $p63^{+/L514F}$ mice and is associated in both, human and mouse AEC keratinocytes, to an impaired regulation of the desmosome genes *Dsp, Dsc3* and *Dsg1* (Ferone et al., 2013).

Unfortunately, $p63^{+/L514F}$ mice die soon after birth because of the cleft palate and this neonatal lethality not allowing either the generation of a mouse line or the study of the adult phenotype (Ferone et al., 2012).

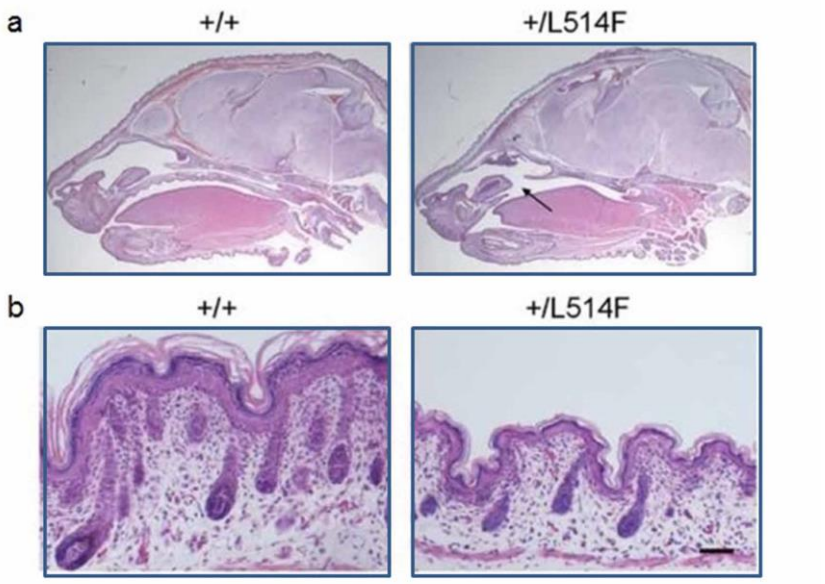

Figure 8. Phenotype of the AEC mouse model p63$^{+/L514F}$. a) Hematoxylin and Eosin staining of sagittal sections of wild type (+/+, left panel) and p63+/L514F (+/L514F, right panel) newborn heads. Cleft of the secondary palate is indicated by the arrow. b) Hematoxylin and Eosin staining of dorsal skin of wild type and p63+/L514F mice at P0. Mutant epidermis is thinner and with less developed hair follicles (adapted from Ferone et al., 2012).

1.7 Quality control of unfolded proteins

The protein quality control (PQC) system consists of multiple chaperone and degradation pathways that cooperate to preserve protein homeostasis (or proteostasis) by ensuring a healthy and functional proteome (Sontag et al., 2017; Houck et al., 2012; Jeng et al., 2015).

Molecular chaperones are proteins that transiently interact with various non-native polypeptides, driving the acquisition of their folded conformation without being associated with them when in their native and functional state (Kampinga et al., 2010). More specifically, they play a crucial role in assisting the folding of

newly synthesized polypeptides to the functional conformation co-traslationally, as they exit the ribosome (Balchin et al., 2016; Chiti and Dobson, 2017). Chaperone functions are not restricted to the protein folding, but include also recognition and sorting of misfolded proteins to the various PQC compartments, by a cooperation with other cellular structures, such as nuclear membrane, ER network and cytoskeleton (Sontag et al., 2017). For example, molecular chaperones can direct specific client proteins towards degradation via both proteasome and autophagy (Howarth et al., 2007; Carra et al., 2008). Importantly, they can stabilize or destabilize interactions between mature, folded proteins (Kampinga et al., 2010).

Nascent polypeptides form folding intermediates when not properly chaperone-assisted toward to their native state. Unfolded intermediates may also accumulate in the case of genetic mutations that impair proper folding or under stress conditions (Chiti and Dobson, 2017) and are often aggregation prone, due to the fact that they typically expose hydrophobic amino acid residues and regions of unstructured polypeptide backbone that are mostly buried in the native state (Hartl et al., 2009). These intermediates can undergo different fates (Fig. 9): they can recover the native conformation by chaperones activity or, if re-folding fails, are degraded via proteosomal or autophagosomal pathways. Alternatively, the unfolded intermediates can form aggregates by self-aggregation or co-aggregation with other unfolded proteins or even with fully folded proteins in the cell (Mogk et al., 2018). Proteins can be recovered from aggregates via disaggregation machines to undergo re-folding or degradation.

The accumulation of newly synthesized, unfolded or misfolded proteins can lead to endoplasmic reticulum (ER) stress, which induces the unfolded protein response of the endoplasmic reticulum (UPR^{ER}) to restore proteostasis (Wang et Kaufman, 2016).

The UPR^{ER} consists of ER transmembrane sensors that are responsive to protein unfolding or misfolding. These sensors can be divided into three branches: inositol-requiring protein 1 (IRE1), protein kinase RNA (PKR)-like ER kinase (PERK) and activating transcription factor 6 (ATF6). Under basal conditions, IRE1, ATF6 and PERK are kept in an inactive state by the binding of a chaperone binding immunoglobulin protein (BiP) to the luminal domains of the sensors. Upon ER stress, BiP is titrated away from UPR sensors and recruited to the unfolded or misfolded proteins, leading to the UPR^{ER} activation (Frakes et al., 2017). More specifically, upon activation, IRE1 ribonuclease directs the splicing of an unconventional 26-nt intron from X-box binding protein 1 (Xbp1) mRNA to generate the spliced xbp1-s isoform, which is translated into a transcription factor involved in regulating the expression of genes such as chaperones. On the other hand, ER stress induces PERK autophosphorylation and homomultimerization. The active phospho-PERK subsequently phosphorylates the α subunit of eukaryotic translation initiation factor 2 (eIF2α), leading to an inhibition of global transcription (Harding et al., 1999). However, phospho-eIF2α preferentially increases the translation of activating transcription factor 4 (ATF4), which activates the transcription of UPR^{ER} and pro-apoptotic genes such as C/EBP homologous protein (Chop) (Marciniak et al., 2004).

A third branch of UPR^{ER}, mediated by ATF6, is activated upon ER stress. After the distruption of the binding to BiP, ATF6 is transported to the Golgi apparatus, where it is cleaved and then transported into the nucleus to induce the expression of Xbp1 and genes involved in ER-associated protein degradation (ERAD) (Yamamoto et al., 2007).

Therefore, the UPR^{ER} plays an essential role in preventing misfolded protein accumulation and consequent aggregation, as it induces cell death if protein misfolding is not resolved.

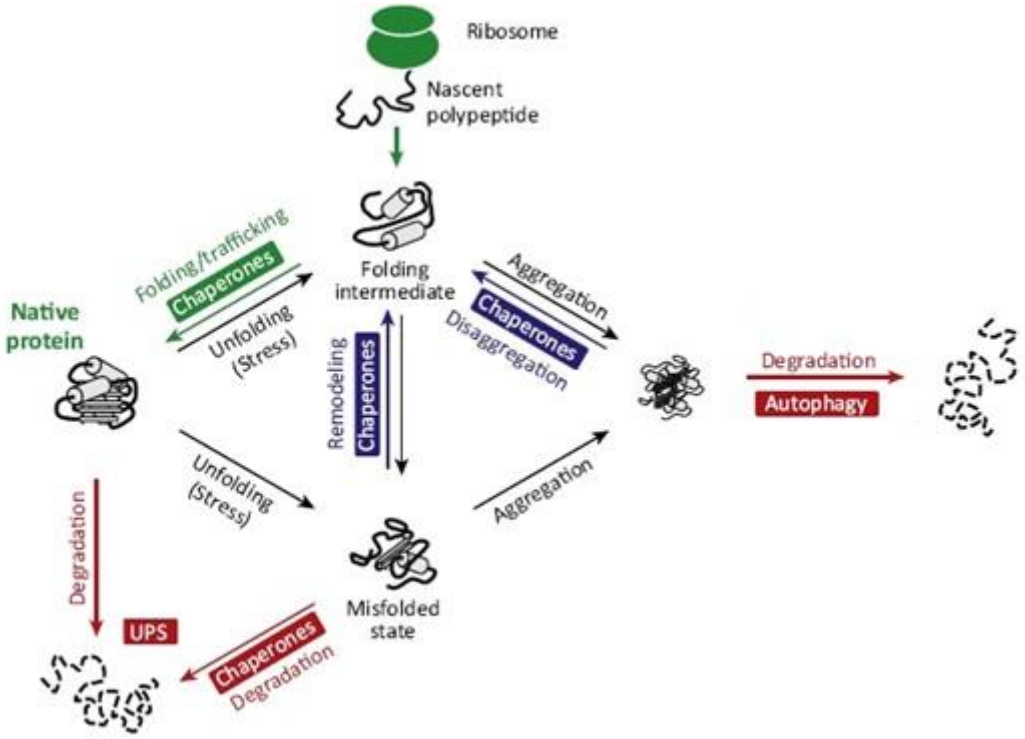

Figure 9. The proteostasis network (PN). The PN consists of three branches aimed to the maintenance of protein homeostasis: biogenesis (in green), conformational maintenance (in blue) and degradation (in red). The nascent polypeptide forms a folding intermediate that, if not properly driven to the native state by chaperones, can turn into a prone-aggregation unfolded or misfolded intermediate. This intermediate can be degraded by the ubiquitin-proteasome system (UPS) or can form toxic or less toxic-amorphous aggregates. The aggregates can be dissolved by the disaggregation machinery and proteins can be directed towards either re-folding or degradation via proteasome. Alternatively, not-dissolved aggregates can undergo autophagic clearance (adapted from Hipp et al., 2014).

1.8 The HSP70 chaperone machine

Protein aggregates can interfere with cellular processes by depleting factors crucial for protein homeostasis (Hipp et al., 2014). Molecular chaperones play a crucial role in preventing unfolded protein aggregation by protecting interactive surfaces against aberrant interactions with other not-canonical molecular partners (Mayer and Bukau, 2005). However, under stress conditions aberrant unfolding proteins may elude the chaperones system control and undergo aggregation. When this happens, cell can respond by different strategies, including disaggregation with recover of the refolded protein or proteasomal degradation and autophagic clearance of protein aggregates (also termed “aggrephagy”; Yamamoto and Simonsen, 2011).

The key component of the disaggregation machinery is the HSP70 chaperone. Heat shock 70 kDa proteins (HSP70s) are ubiquitous molecular chaperones that function in a myriad of biological processes, including polypeptide folding, degradation, translocation across membranes and protein–protein interactions (Kampinga et al., 2010). Given its mutifunctionality, HSP70 never works alone, but its activity is driven by a class of cofactors: the J proteins, also known as HSP40s. Historically, J proteins have been divided into three classes (known as DNAJA, DNAJB and DNAJC), although this classification does not reflect either the biochemical function or the mechanism of action of group members, but rather is based on shared domains and motives (Hageman et al., 2009).

Generally, the J proteins orchestrate HSP70 functions by delivering specific client proteins to HSP70 in precise locations in the cell, thus determining their fate. Often multiple J proteins function with a single HSP70, performing different activities.

According to the “canonical model” of the HSP70 machinery (Szabo et al., 1994; McCarty et al., 1995; Laufen et al., 1999), J protein initially binds the unfolded client protein preventing its aggregation and delivers it to HSP70, stimulating also HSP70 ATPase activity. Then a nucleotide exchanging factor (NEF) binds to HSP70 causing the release of ADP and the subsequent binding of a new molecule of ATP. ATP binding induces an HSP70 conformational change leading to the release of the client protein and the loading of a new J protein-unfolded client complex and the cycle begins again.

In metazoa, HSP70 exhibits an autonomous disaggregation activity, supported by class A and B-type DNAJ-proteins that enhances loading of HSP70 at the aggregate surface. HSP70 can favor the release of trapped polypeptides from the aggregate applying pulling forces and moving away from the aggregate. Binding of Hsp110, that acts as a NEF, recycles HSP70 to initiate new binding and pulling events (Mogk et al., 2018; Fig.10).

Interestingly, some J proteins localize in precise compartments of the cell where they perform specific functions also in an HSP70-independent manner. More specifically, members of a subclass of the DNAJB family (particularly DNAJB6b and DNAJB8) act as suppressors of aggregation and toxicity of disease-associated polyglutamine proteins and their anti-aggregation activity is performed also in the absence of HSP70 (Hageman et al., 2010). DNAJB6 is found into two isoforms: the shorter isoform (DNAJB6b) is present in both the nucleus and the cytosol, while the longer isoform (DNAJB6a) is exclusively nuclear (Hanai and Mashima, 2003) and displays effective anti-aggregation properties only on nuclear aggregates (Hageman et al., 2010).

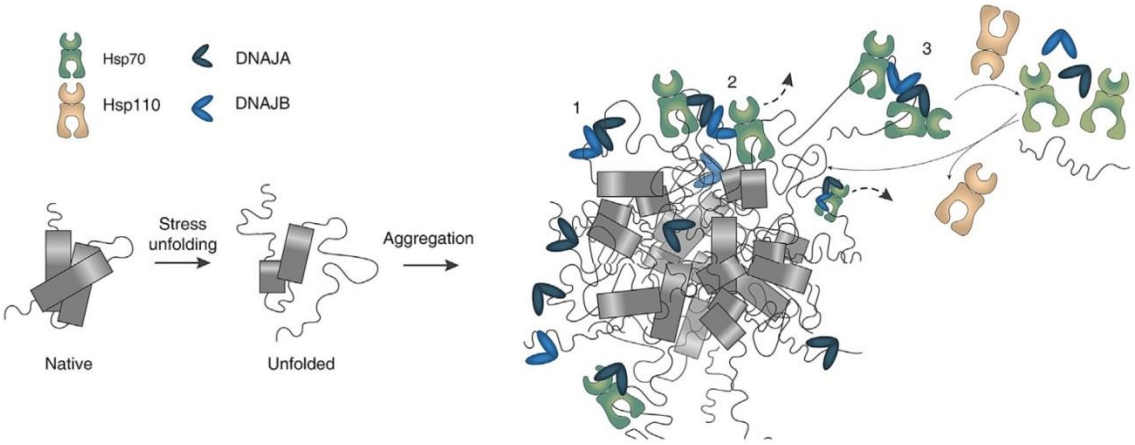

Figure 10. HSP70 Disaggregation Machinery. Unfolding stress conditions like heat shock can cause protein unfolding and the formation of amorphous aggregates. A bi-chaperone system formed by Hsp70 and HSP110, with the cooperation of DNAJA and DNAJB co-chaperones, solubilizes aggregated proteins. First, J proteins bind the aggregate (1), then recruit HSP70 at the aggregate surface (2). HSP70 moves away from the aggregate promoting the release and the folding of trapped polypeptides. Finally, HSP110 binds HSP70 and allows its recycle for a new disaggregation event (3) (adapted from Mogk et al., 2018).

2. AIM OF THE STUDY

My research activity was aimed to investigate the molecular mechanisms underlying the AEC syndrome, focusing on the structural and functional alterations of the transcription factor p63 in the presence of the AEC-causative mutations. More specifically, I evaluated the effects of these mutations on p63 protein conformation, transcriptional activity and DNA binding ability.

In the second part of my work, I investigated potential approaches to specifically target the aberrant molecular events underlying the AEC phenotype, in order to lay the foundation for a therapeutic strategy. To this aim, I evaluated to strengthening the activity of the endogenous protein quality control system specifically towards the AEC mutant p63 protein.

3. MATERIALS AND METHODS

3.1 Primary mouse keratinocytes isolation and cell cultures

Primary keratinocytes were isolated from the epidermis of newborn mice. 2-3 days old mice were euthanized by hypothermia by placing them in a 100mm Petri Dish under ice for 30-45 minutes. Then mice were washed once with distillated water and twice with 70% ethanol, being careful to remove completely the ethanol after washing. The skin was removed from each mouse under a tissue culture hood using first sterile surgical scissors to amputate the limbs and the tail and then a sterile scalpel to cut the skin along the dorsal midline from the head to the tail. Using sterile forceps, the whole skin was removed, washed in HBSS and flatten with the dermis down on a petri dish. Then the skin was incubated overnight at 4°C floating on 2 ml of Dispase solution (0.80 U/mL Dispase II, 10 mM HEPES, 0.075% sodium bicarbonate, antibiotic/ antimycotic in HBSS) to obtain epidermis-dermis dissociation. Next day the epidermis was peeled away from dermis with forceps, placed in 2 ml of trypsin solution (0.125% trypsin, 0.1 mM EDTA in HBSS) and cut quickly into very small fragments with scissors to promote the enzymatic and mechanical dissociation of the tissue. The minced epidermis was incubated at 37°C for 5 minutes. Then trypsin was inactivated by adding DMEM medium supplemented with 10% of FBS and the cell suspension was filtered in 70 μm cell strainer to remove undigested tissue and floating fragments. The isolated keratinocytes were plated in collagen coated dishes in high calcium medium to enhance cell attachment. Next day, keratinocytes were washed twice with PBS to remove unattached cells and calcium residuals and grown at 34°C and 8% CO_2 in low calcium medium (0.05 mM $CaCl_2$) supplemented with 4% of calcium-chelated

Fetal Bovine Serum (FBS) and Epidermal Growth Factor (EGF), changing medium every day.

Neonatal HDFn, H1299, HEK293T and Saos-2 cells were cultured in Dulbecco's Modified Eagle Medium (DMEM) supplemented with 10% FBS. Human primary keratinocytes HK, NHEK and AEC were grown in Epilife medium (Thermo Fisher Scientific).

3.2 Mouse genotyping

The conditional knock-in L514F mutant mice $p63^{+/FloxL514F}$, $p63^{FloxL514F/FloxL514F}$, K14Cre;$p63^{+/FloxL514F}$ (+/L) and K14Cre;$p63^{FloxL514F/FloxL514F}$ (L/L) genotyping was performed by PCR using DNA isolated from mouse tails.

The oligonucleotides primers used for the screening of FloxL514F allele are:

Forward primer (5'-3'): CAGCGTATCAAAGAGGAAGGAGA

Reverse primer (5'-3'): AGCCAGAATCAGAATCAGGTGAC

A 250bp band is expected for the wild-type mice, a 337bp band for the mutant homozygous mice and both bands for the heterozygous ones.

To screen mice for the presence of Cre-recombinase, the following oligonucleotides primers were used:

Forward primer (5'-3'): GGCAGTAAAAACTATCCAGCAACA

Reverse primer (5'-3'): TAACATTCTCCCACCGTCAGTA

A 300bp band is expected for the K14Cre mice.

3.3 Adenoviral infection

Confluent primary keratinocytes (10^6 cells in 60mm dish) newly-isolated from $p63^{+/FloxL514F}$ or $p63^{FloxL514F/FloxL514F}$ conditional knock-in mice were infected 5 days after plating with adenovirus carring Cre-recombinase or GFP as control at MOI 100 (provided by Okairos). Cells were incubated with the adenovirus for 2h at 34°C and 8% CO_2 in serum-free low calcium medium (1.2 ml of medium for a 60mm dish). Then LCM supplemented with serum and EGF was added to the adenovirus mix up to a volume of 3 ml and left overnight at 34°C and 8% CO_2. Next day the adenovirus was removed and fresh medium was added. Cells were collected 4 days after infection.

3.4 Retroviral preparation

High-titer retroviruses were produced in HEK293T cells by transient co-transfection of pBABE p63 constructs or pMXs-KLF4 plasmid and amphotropic viral envelope plasmid (pAmpho). Cells were plated on collagen coated-60mm dishes the day before transfection. Subconfluent cells were co-transfected using 6μg of pBABE or pMXs constructs and 6μg of pAmpho plasmid in the presence of 30ul of Lipofectamine 2000 (Thermo Fisher Scientific), according to the manufacturer's instructions. Cell supernatants containing the retroviruses were collected 48 hr after transfection, then fresh medium was added and collected again 72 hr after transfection. Finally, the retrovirus preparation was filtered using 0.45μm filters to remove cell debris.

3.5 Retroviral infection

Mouse primary keratinocytes newly-isolated from wild type mice (C57BL/6 strain) were infected the day after plating at 50% confluence in 35mm dish with retroviruses carrying p63, produced as described above, in the presence of 8 μg/ml Polybrene. Cells were incubated in the retrovirus mix for 2 hr at 34°C and 8% CO_2. Since retroviruses were produced in the high-calcium medium of HEK293T cells, keratinocytes were washed twice with PBS after infection to remove calcium residuals and then low calcium medium was added.

Cells were infected for two consecutive days and 48h after the second infection were selected with 1μg/ml puromycin. After 48 hr uninfected control keratinocytes were died and infected cells were collected for RT-qPCR and Western blot analysis.

3.6 HDFn-to-iKCs conversion assay

2.4 x 10^6 neonatal HDFs were plated in 35mm dish and co-infected at 30% confluence, the day after plating, with retroviruses carrying p63 and KLF4 (Chen et al., 2014) in the presence of 8 μg/ml Polybrene. Cells were incubated in the retrovirus mix for 2 hr at 37°C. The next day a second infection was performed. Cells were then splitted into two 60mm dishes and selected with 2 μg/ml puromycin 48 hr after the second infection, changing medium supplemented with puromycin at alternate days until the uninfected control cells were died (48 hr after the start of selection). HDF-to-iKCs conversion was assessed 18 days after selection by RT-qPCR and Western blot analysis.

3.7 RNA isolation and RT-qPCR

Total RNA was extracted from cells using TRIzol reagent (Thermo Fisher Scientific) and retro-transcribed to cDNA using SuperScript Vilo (Thermo Fisher Scientific). RT-qPCR was performed using the SYBR Green PCR master mix (Thermo Fisher Scientific) in an ABI PRISM 7500 (Thermo Fisher Scientific). Target genes were quantified using the following specific oligonucleotide primers and normalized for human RPLP0 expression or for mouse β-actin expression:

Oligonucleotide primers for Real Time RT-PCR		
Gene	**Forward 5'-3'**	**Reverse 5'-3'**
hRPLP0	GACGGATTACACCTTCCCACTT	GGCAGATGGATCAGCCAAGA
hKRT14	GGATGACTTCCGCACCAAGT	TCCACACTCATGCGCAGGT
hIRF6	CAGCTCTCTCCCCATGACTGA	CCCATACTCCTTCCCACGATAC
mβ-act	CTAAGGCCAACCGTGAAAAGAT	GCCTGGATGGCTACGTACATG
mKrt5	CAACGTCAAGAAGCAGTGTGC	TTGCTCAGCTTCAGCAATGG
mKrt14	GATGTGACCTCCACCAACCG	CCATCGTGCACATCCATGAC
mDsc3	CCACCGTCTCTCACTACATGGA	TGTCCTGAACTTTCATTATCAGT TTGT
mIrf6	CAGCTCTCTCCCCATGACTGA	CCCATACTCCTTCCCACGATAC
mFgfr2	TGGATCGAATTCTGACTCTCACA	TTCGAGAGGCTGGGTGAGAT
mSmad7	AACGAGAGTCAGCACTGCCA	GAAGGTGGTGCCCACTTTCA
mKrt8	TGCTCATGTTCTGCATCCCA	GATCACCACCTACCGCAAGC

3.8 ChIP-qPCR

For Chromatin immunoprecipitation (ChIP), 3 x 10^6 HEK293T cells were fixed with 1% formaldehyde in growth medium at 37°C for 10 minutes. Extracts were extensively sonicated with BIORUPTOR (Diagenode) at 4°C to obtain DNA fragments ranging from 400 to 800 bp in length. Chromatin was immunoprecipitated using rabbit antibodies for p63 (H-137; Santa Cruz Biotechnology) or rabbit IgG (Santa Cruz Biotechnology) as negative control. Bound chromatin was purified with Protein A Sepharose for 1hr at 4°C and then p63 binding sites in human KRT14 promoter were quantified by RT-qPCR using the following specific oligonucleotide primers and normalized to input (total chromatin):

Forward primer (5'-3'): GGGCCTGTCTGAGGAGATAGG

Reverse primer (5'-3'): AGGCATGTTGAGAGGAATGTGA

3.9 BN-PAGE, SDS-PAGE and Western Blot

For BN-PAGE H1299 cells or mouse primary keratinocytes were scraped on ice in Native lysis buffer (25 mM Tris (pH 7.5), 150 mM NaCl, 2 mM MgCl2, 20 mM CHAPS, 1 mM DTT and protease inhibitors), collected and incubated 1h in ice in the presence of benzonase (Merck) for lysis and digestion of nucleic acids. Native lysates were then mixed with 20% Glicerol and 5mM Comassie G-250 and loaded on 3–12% Novex Bis-Tris gradient gel for BN-PAGE (NativePAGE system, Thermo Fisher Scientific), according to the product manuals. For SDS-PAGE, lysates were prepared in Laemmli buffer (10% glycerol, 0.01 % Bromophenol Blue,

0.0625 M Tris-HCl pH 6.8, 3 % SDS, 5 % ßmercaptoethanol), boiled and loaded on denaturing SDS-PAGE gel. To isolate nuclear and cytoplasmic extracts from keratinocytes, the extraction kit “NE-PER™ Nuclear and Cytoplasmic Extraction Reagents” (Thermo Fisher Scientific) was used following the manufacturer’s instruction. Protein concentration was then measured by Bradford assay and 8ug of each extract, nuclear or cytoplasmic, were loaded for SDS-PAGE. For Western Blot, proteins were transferred after run to Immobilon-P transfer membranes (Millipore) and probed with the antibodies diluted in PBS-0.2% Tween-20 with 5% nonfat-dry milk. The primary antibodies used for Western Blot analysis were: anti-p63 (EPR5701), (Santa Cruz Biotechnology), anti-Keratin 14 (Covance), anti-ERK1 (Santa Cruz Biotechnology) anti-ß-Actin (AC-15, Santa Cruz Biotechnology), anti-IRF6 (Ferone et al., 2012), anti-p53 (Ab6) Pantropic DO-1 (Millipore), anti-PARP1 (Cell Signaling), anti-α-Tubulin (Sigma-Aldrich), anti-HSP70/HSC70 (W27) (Santa Cruz Biotechnology), anti-V5 (Thermo Fisher Scientific), anti-FLAGM2 (Sigma-Aldrich). The following primary antibodies were diluted in TBS-0.2% Tween-20 with 5% Bovine Serum Albumin: anti-phospho-PERK(Thr980) (Cell Signaling), anti-eIF2α (Cell Signaling), anti-phospho-eIF2α(Ser51) (Cell Signaling), anti-ATF-4(EPR18111) (Cell Signaling), anti-GADD 153 (B-3) (*Chop*) (Santa Cruz Biotechnology). Secondary antibodies donkey anti-rabbit or sheep anti-mouse IgG conjugated to horseradish peroxidase (HRP) (GE Healthcare) were used and revealed by chemiluminescence (ECL, GE Healthcare Life Sciences).

3.10 Luciferase reporter assay and p53-p63 DNA binding competition assay

Luciferase assays in HEK293T cells were performed using the reporter constructs K14 promoter-luc (Candi et al., 2006) or FGFR2 enhancer-luc (Ferone et al., 2012), that carry firefly luciferase gene under the control of Keratin 14 promoter and FGFR2 enhancer, respectively. 70% confluent cells were co-transfected in 24-well dishes with the reporter construct and the plasmid encoding wild type or mutated ΔNp63α at a ratio 1:3, using Lipofectamine 2000 (Thermo Fisher Scientific) following the manufacturer's instruction.

p53-p63 DNA binding competition assay was performed in Saos-2 cells using the reporter construct pG13Luc (el-Deiry et al., 1993), carrying firefly luciferase gene under the control of a p53 binding site that efficiently binds both p53 and p63, but is activated only by p53 and not by ΔNp63α (McGrath et al., 2001). 70% confluent cells were co-transfected in 24 well dishes with 125ng of pG13Luc plasmid and 20ng of pFLAG-CMV2-p53 with or without pFLAG-CMV2-ΔNp63α at different concentrations (10ng, 20ng or 40ng) using Lipofectamine 2000 (Thermo Fisher Scientific).

In all the luciferase assays, *Renilla* Luciferase Vector (pRL-CMV; Promega) was co-transfected and *Renilla* activity was used to normalize transfection efficiency. Luciferase and *Renilla* activities were measured in the same sample 48 hr after transfection using the dual-luciferase reporter assay kit (Promega).

3.11 Co-Immunoprecipitation

HEK293T cells were plated in collagen-coated 35mm dishes and co-transfected at 95% confluence the day after plating with 1.5 μg of pFLAG-CMV2-

ΔNp63a (wild type or mutant) plasmid and 1.5 μg of pcDNA5-FRT/TO V5 DNAJB1 or DNAJB6a or DNAJB6b plasmid, using Lipofectamine 2000 (Thermo Fisher Scientific). After 48 hr, cells were washed twice with PBS and lysed in 500mL of Intermediate lysis buffer (50mM Tris-HCl pH 8, 150mM NaCl, 0.5% NP-40) with fresh-added protease and phosphatase inhibitors for 15 minutes on ice.

Lysates were collected with a scraper and centrifuged at maximum speed for 10 minutes at 4°C, to remove cellular debris. Supernatants were collected and 10% of total lysate (Input) was kept for normalization. The immunoprecipitation was performed on the remaining lysate by adding 15 μl packed-gel volume of anti-FLAG M2 conjugated to agarose beads (Sigma), supplied 50% slurry and equilibrated with the Intermediate buffer just prior to use. After 2 hours of incubation in rotation at 4°C, unbound fraction was collected and the beads were washed 4 times with Intermediate lysis buffer plus PMSF and protease inhibitors. Finally, immunoprecipitated fraction was eluted by resuspension of the beads in Laemmli buffer 2X (20% glycerol, 0.02 % Bromophenol Blue, 0.125 M Tris-HCl pH 6.8, 6 % SDS) and incubation at 65°C for 5 minutes. Samples were centrifugated and the supernatant was transferred in new tubes to discard the beads.

For HSP70-p63 co-immunoprecipitation, H1299 were transfected at 95% confluence in 35mm dishes with 2 μg of pcDNA3.1-ΔNp63α (wild type or mutant) plasmid, using Lipofectamine 2000 (Thermo Fisher Scientific). After 24 hours, cells were washed and lysed as described above. 10% of Input was kept and the remaining lysate was incubated with anti-HSP70/HSC70 (W27) monoclonal antibody (Santa Cruz Biotechnology) overnight at 4 °C in rotation. Bound proteins were immunoprecipitated by incubation with Protein A Sepharose for 1hr at 4°C in rotation. The collection of HSP70-bound proteins was performed as described above.

3.12 Differentiation and PRIMA-1-Met and STIMA-1 treatment of human epidermal keratinocytes

Keratinocytes were cultured at low density in Epilife medium with Human Keratinocyte Growth Supplement (HKGS). The differentiation process *in vitro* occurred when cells reached the full confluence (covering 100% of the dish area). When keratinocytes became 100% confluent, the Epilife growth medium was swiched to Epilife medium supplied with 1.5 mM $CaCl_2$, to sustain differentiation, and replaced every two days with fresh medium. Differentiated keratinocytes were observed at microscope taking pictures at different time points (3, 5, 7, 10 days of differentiation) to assess morphological changes.

For PRIMA-1-Met / STIMA-1 treatments, subconfluent normal human epidermal keratinocytes (NHEK) or human keratinocytes derived from an AEC patient (AEC keratinocytes) were treated with PRIMA-1-Met 30 μM and/or STIMA-1 10 μM in Epilife medium with HKGS. After 48 hours they reached 100% confluence and the differentiation process started, sustained by the addition of 1.5mM $CaCl_2$ to the growth medium. The growth medium was replaced every two days with fresh medium containing $CaCl_2$ and PRIMA-1-Met/ STIMA-1 compounds at the concentrations indicated above and keratinocytes were observed at the microscope taking pictures 10 days later.

4. RESULTS

4.1 Mutations in p63 causative of AEC syndrome impair p63 transcription function

P63 mutations causative of AEC syndrome cluster mainly in the carboxyl-terminal domains of the protein and include missense mutations (e.g. L514F, C519R, G530V, D544Y in the SAM domain or R598L and D601V in the TI domain) and frameshift mutations that lead to abnormal extensions (e.g. 1709DelA, 1859DelA, 3'ss intron 10, 1456InsA) of the protein. Mutations causative of other p63 syndromes are usually found in different sites along the protein and are likely to affect p63 function by different mechanisms. More specifically, EEC-associated mutations (e.g. R304Q) are mainly located in the DNA binding domain, thus compromising p63 binding to the DNA.

To investigate the effect of AEC-associated mutations on p63 transcriptional functions we firstly tested the ability of a group of p63 mutants to transactivate the keratin 14 (KRT14) promoter by performing a luciferase reporter assay in HEK293T cells (Fig.11). As previously reported (Candi et al., 2006), ΔNp63α efficiently transactivated KRT14 promoter, whereas the EEC-associated mutant R304Q lost this function. All the tested AEC-associated mutations displayed an impaired transactivation ability. Interestingly, two missense mutations falling in the TI domain (Q630X, E635X) that are causative of SHFM retained the transactivation activity, indicating that they could affect p63 functions in other contexts or with alternative mechanisms.

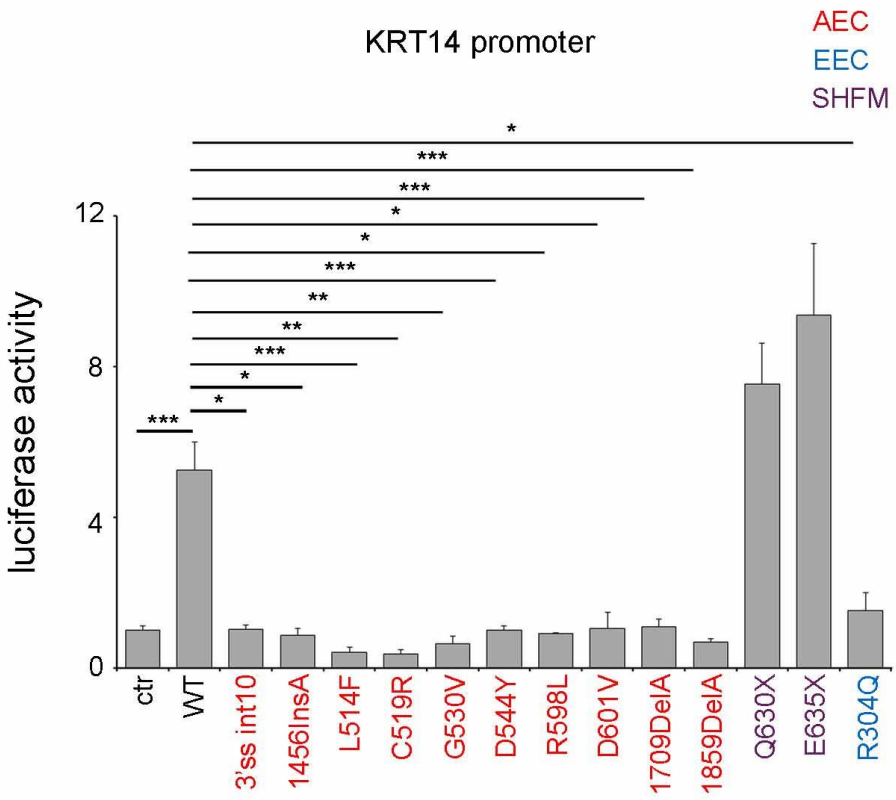

Figure 11. Transactivation activity of wild type p63 and p63 mutants. Luciferase reporter assay in HEK293T cells co-transfected with wild type p63 or the indicated p63 mutants and the reporter vector carrying the firefly luciferase gene under the control of K14 promoter at a ratio 3:1. A *Renilla* luciferase control vector was co-transfected. Firefly and *Renilla* luciferase activities were measured sequentially from a single sample and *Renilla* luminescence was used to normalize firefly luminescence. (n=11). Data are shown as mean of independent samples ± standard error of the mean (SEM). Statistical significance was assessed using one-way ANOVA analysis. * $p \leq 0.05$; **; $p \leq 0.001$; *** $p \leq 0.0001$.

To assess whether AEC mutations similarly affect p63 transcriptional activity in a more physiological context, as in epidermal keratinocytes, we took advantage of a conditional knock-in mouse model for AEC syndrome ($p63^{+/floxL514F}$) generated in our laboratory, in which the AEC mutation L514F in exon 13 is expressed only in

the presence of the Cre recombinase. More specifically, the wild type exon 13 is replaced with mutant exon 13 upon Cre recombinase deletion (Fig.12).

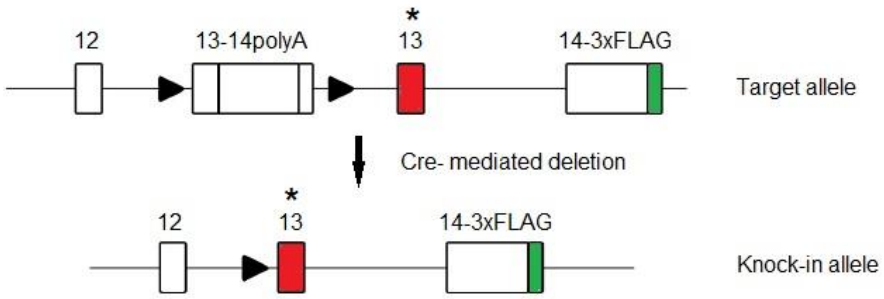

Figure 12. Gene targeting strategy used for the generation of p63+/L514Fflox knock-in mice. Schematic representation of target and knock-in alleles of $p63^{+/L514Fflox}$ mice. L514F mutation in exon 13 is indicated with *. In the target allele, LoxP sites (black triangles) flank wild-type exon 13 fused with the coding portion of exon 14 and the SV40 polyA (13-14polyA, upper). Mutant exon 13 (in red) was placed downstream LoxP sites and 3xFLAG (in green) was added at the end of the coding sequence of exon 14 located downstream the mutant exon 13 (14-3xFLAG). FLAG-tagged p63 mutant protein is expressed upon Cre-mediated deletion of 13-14polyA portion (knock-in allele, lower).

The conditional knock-in strategy allows to overcome the neonathal lethality due to cleft palate observed in the constitutive knock-in mouse model (p63+/L514F), previously generated in our laboratory (see Introduction section). To study the evolution of the skin phenotype in AEC mice, we crossed $p63^{L514Fflox/L514Fflox}$ mice with K14-Cre knock-in mice carrying the Cre recombinase gene under the control of the endogenous Krt14 promoter, that is active in stratified epithelia from embryonic day 17.5 (Huelsken et al., 2001). The generated

K14-Cre; p63$^{L514Fflox/L514Fflox}$ homozygous mice (L/L) fully recapitulate the skin defects and erosions found in AEC patients (Fig.13).

Figure 13. Phenotype of K14-Cre; p63$^{L514Fflox/L514Fflox}$ mice. Upper panel: newborn K14-Cre; p63$^{L514Fflox/L514Fflox}$ (L/L) mouse lacking of a large area of skin (representative of 10% of L/L mice at P0). Lower panel: wild type and L/L mice at P7. The mutant mouse displays skin crusting and erosions, with reduced body size and dehydratation (representative of 100% of L/L mice at P7-P8).

In addition, we measured the expression levels of epithelial p63 target genes in primary keratinocytes isolated from heterozygous p63$^{+/L514Fflox}$ and homozygous p63$^{L514Fflox/L514Fflox}$ mice, after infection with adenoviruses carrying the Cre recombinase (adeno-Cre) or the GFP (adeno-GFP) as control. Both real time RT-PCR and Western blot analysis revealed that the expression of several genes known to be positively regulated by p63, including Krt14, Krt5, Fgfr2, Irf6 and Dsc3 (Ferone et al., 2012; Ferone et al., 2013), were strongly reduced in homozygous keratinocytes (p63$^{L514Fflox/L514Fflox}$) and to a lesser extent in heterozygous keratinocytes (p63$^{+/L514Fflox}$), upon adeno-Cre infection (Fig.14A-B). Interestingly,

the expression of genes repressed by p63, such as Smad7 and Krt8 (De Rosa et al., 2009), was activated in the presence of the L514F mutation compared to the control (Fig. 13C), thus demonstrating that both transactivation and repression functions of p63 are impaired by AEC mutations.

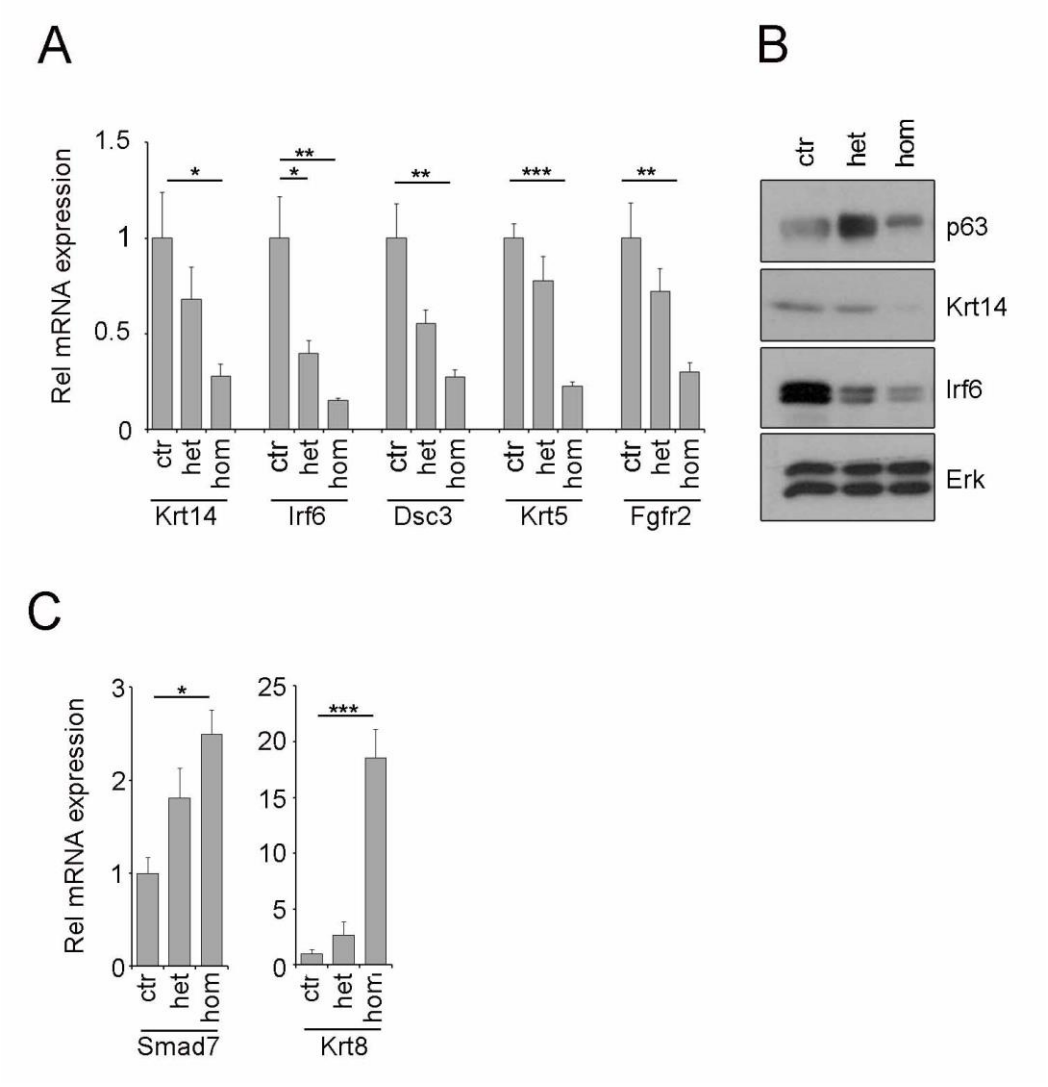

Figure 14. Transcriptional activity of heterozygous and homozygous p63L514F mutant compared to wild type p63 in mouse primary keratinocytes. A) Real time RT-PCR of target genes induced by p63 in primary keratinocytes derived from $p63^{+/floxL514F}$ (het) and $p63^{floxL514F/floxL514F}$ (hom) mice, after infection with adenoviruses carrying Cre recombinase or GFP (ctr) (n=5). B) SDS-PAGE followed by Western blot for p63 and its target genes Krt14 and Irf6 in primary mouse keratinocytes treated as in (A). Erk was used as loading control. C) Real time RT-PCR of target genes repressed by p63 in primary mouse keratinocytes treated as in (A) (n=3). In (A) and (C) mRNA levels are normalized to

β-actin expression. Ctr mRNA levels are set to 1. Data are shown as mean ± SEM. Statistical significance was assessed using one-way ANOVA analysis. *p ≤ 0.05; **p ≤ 0.001; ***p ≤ 0.0001.

4.2 AEC-associated mutations partially reduce p63 DNA binding ability

We next investigated the causes of the impaired transcriptional activity observed in AEC-associated p63 mutants. To this aim, we tested the ability of AEC mutants to bind DNA by performing chromatin immunoprecipitation (ChIP) experiments with anti-p63 (H137) antibody in HEK293T cells transfected with wild type or mutant p63. P63 binding sites on KRT14 promoter were quantified by quantitative PCR (q-PCR) in the p63-bound chromatin and normalized to input. As previously reported, the EEC-associated mutant R304Q did not bind to well-characterized p63 genomic binding sites in KRT14, whereas SHFM-associated mutants Q630X and E635X retained the DNA binding ability. Surprisingly, AEC mutants displayed a reduced binding to DNA, although AEC mutations do not affect directly the DNA binding domain (Fig.15).

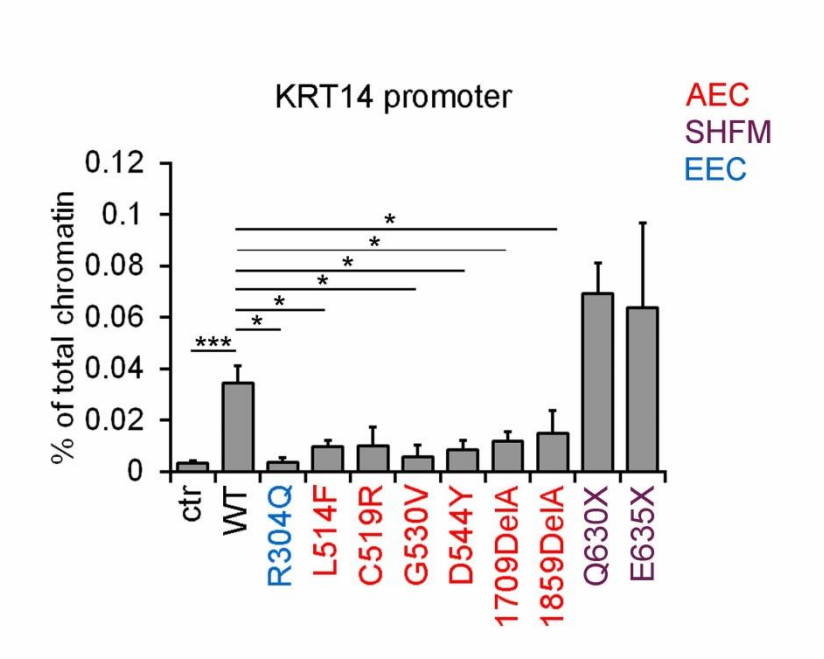

Figure 15. DNA binding ability of wild type p63 and AEC-associated p63 mutants. ChIP-qPCR in HEK293T cells overexpressing p63 wild type and the indicated p63 mutants on the KRT14 promoter (n=6). Immunoprecipitation was performed with anti-p63 (H137) antibody and p63-bound chromatin was analyzed by qPCR using specific primers for p63 binding sites in KRT14 promoter. EEC-associated mutant R304Q was used as negative control. Data are calculated as percentage of total chromatin targeted by primers and are shown as mean of independent experiments ± SEM. Statistical significance was assessed using one-way ANOVA analysis. *p ≤ 0.05; **p ≤ 0.001; ***p ≤ 0.0001.

To further characterize the DNA binding ability of AEC mutants, we performed a p53-p63 DNA binding competition assay using the pG13Luc reporter construct containing the firefly luciferase gene under the control of a p53 binding site that is efficiently bound by both p53 and p63, but luciferase expression is activated only by p53 and not by ΔNp63α (McGrath et al., 2001). Saos-2 cells, that are devoid of endogenous p53 and p63, were co-transfected with a fixed p53 concentration and increasing concentrations of p63 wild type or mutant in the presence of pG13-Luc

reporter construct. As expected, wild type p63 competed with p53 strongly impairing its transactivation activity, whereas the EEC mutant R304Q, being unable to bind to DNA, did not interfere with p53 transactivation at any tested concentration. On the other hand, AEC mutants L514F, D544Y and 1859DelA prevented p53 binding to DNA in a dose-dependent manner, indicating that they retained the ability to bind DNA, albeit with reduced efficiency compared to wild type p63 (Fig.16A). Samples were analyzed for Western blot to control p53 and p63 expression (Fig.16B).

Taken together, these results indicate that the DNA binding ability of AEC mutants is not intrinsically impaired, but rather is weakened, likely due to structural alterations.

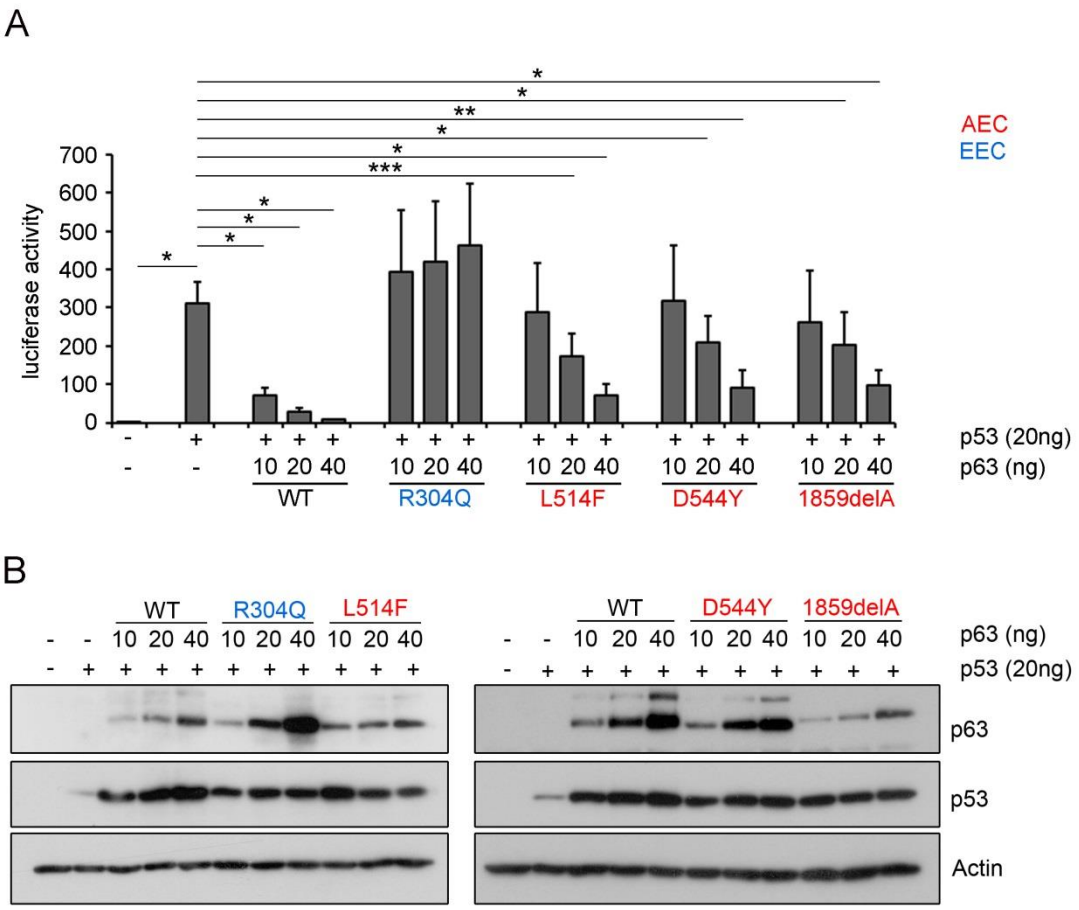

Figure 16. DNA binding competition with p53 of wild type p63 or AEC-associated p63 mutants at increasing doses. A) Luciferase reporter assay in Saos-2 cells co-transfected with p53 and wild type or mutant p63 at 2:1, 1:1 or 1:2 ratios in the presence of pG13-luc reporter construct. A *Renilla* luciferase control vector was co-transfected. Data were normalized for *Renilla* luciferase activity (n=3). Data are shown as mean ± SEM. Statistical significance was calculated using paired one-tailed *t* test. *p ≤ 0.05; **p ≤ 0.01; ***p ≤ 0.001. B) SDS-PAGE followed by Western blot for p53 and p63 of the samples shown in (A). β-actin was used as loading control.

4.3 AEC-associated p63 mutant proteins form large aggregates in keratinocytes

To deepen the mechanism by which AEC-associated mutations interfere with p63 functions we investigated the structural alterations specifically caused by AEC mutations, which exhibit a well-defined genotype-to-phenotype correlation.

NMR studies performed in collaboration with the laboratory of Professor Volker Dötsch (Institute of Biophysical Chemistry, Goethe University of Frankfurt, Germany) revealed that AEC-associated p63 mutation L514F caused a less compact fold of the protein, leading to a destabilization of the SAM domain. In addition, p63L514F protein displayed a lower melting temperature and irreversibly precipitated upon unfolding induced by high temperature, in contrast to wild type p63, whose unfolding was reversible (data not shown). Importantly, these observations were associated to an increased aggregation propensity found in several AEC mutant p63 proteins analyzed using the TANGO algorithm, which predicts aggregation prone regions (APRs) in an amino acidic sequence.

Next, we verified if protein aggregation occurred in AEC mutants endogenously expressed in epidermal keratinocytes. To this aim, we took material from the $p63^{+/floxL514F}$ knock-in mouse model for AEC syndrome, available in our laboratory, and from a patient affected by AEC syndrome, thanks to a collaboration with Prof. Daniel Aberdam (INSERM, Paris, France), who provided us the human keratinocytes.

We performed BN-PAGE on keratinocytes lysates prepared in native conditions, followed by Western blot analysis for p63. As expected, in mouse keratinocytes derived from $p63^{+/floxL514F}$ and infected with adeno-GFP, wild type p63 mainly runs as a monomer. In contrast, in adeno-Cre–infected $p63^{+/L514Fflox}$ keratinocytes two forms were observed: the monomeric one and a large multimeric

assembly at high molecular weight (from 480 to 1048 KDa), which may referred to as “protein aggregate”. Finally, in Ad-Cre–infected p63$^{L514Fflox/L514Fflox}$ keratinocytes the monomeric form was lost and only the aggregated form was visible (Fig.17A). Similar results were observed in primary keratinocytes derived from Krt14-Cre;p63$^{+/L514Fflox}$ and Krt14-Cre;p63$^{L514Fflox/L514Fflox}$ mice compared with wild type controls p63$^{+/L514Fflox}$ (Fig.17B). In AEC human keratinocytes, carrying the p63 mutation T537P in heterozygosity, both the monomeric and the aggregated forms were detected. Conversely, in primary adult human keratinocytes (HK) and neonatal human keratinocytes (NHEK), both used as controls, wild type p63 run mainly as monomer (Fig.17C).

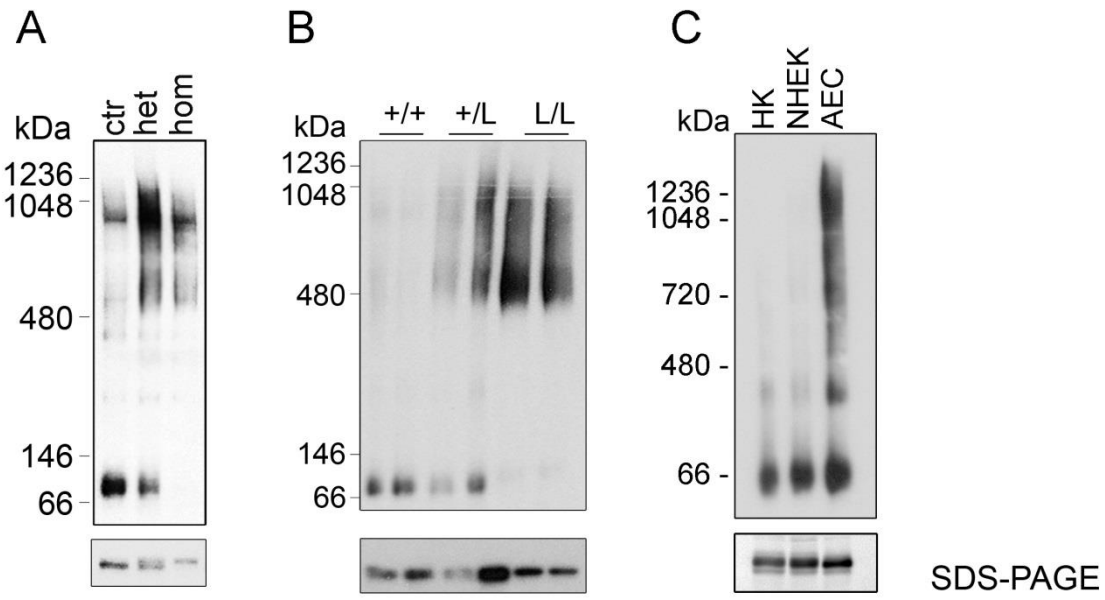

Figure 17. Protein aggregates formed by AEC mutants in mouse and human primary keratinocytes. BN-PAGE (upper) and SDS-PAGE (lower) followed by Western blot for p63 on native lysates of primary keratinocytes. A) Primary keratinocytes derived from p63$^{+/floxL514F}$ (het) and p63$^{floxL514F/floxL514F}$ (hom) mice, after infection with adenoviruses carrying Cre recombinase or GFP (ctr). B) Primary keratinocytes derived from p63$^{+/floxL514F}$ (+/+), K14-Cre; p63$^{+/floxL514F}$ (+/L) and K14-Cre; p63$^{floxL514F/floxL514F}$ (L/L) mice. (C) Adult human keratinocytes (HK), normal human epidermal keratinocytes (NHEK) and primary

keratinocytes derived from an AEC patient carrying the heterozygous p63 mutation T537P (AEC).

4.4 Transcriptional activity is restored by reducing the aggregation propensity of AEC-associated p63 mutant proteins

In collaboration with Prof. Volker Dötsch we identified in p63 wild type and in some AEC-associated p63 mutants the aggregation-prone regions (APRs) using the TANGO algorithm. The analysis of wild type p63 sequence revealed a peak of β-aggregation propensity in the TI domain, which was abolished when the substitution V603D was introduced (Fig.18B). The frameshift mutations 3'ss intron 10, 1709DelA and 1809DelA caused the introduction of new aggregation-prone sequences (Fig.18A), whereas the missense mutations R598L and D601V led to an increase in the intrinsic aggregation propensity of the TI domain (Fig.18B). Therefore, the biochemical analysis of AEC-associated mutants indicated that the AEC mutations caused an alteration of p63 protein conformation leading to the exposure of aggregation-nucleating sequences.

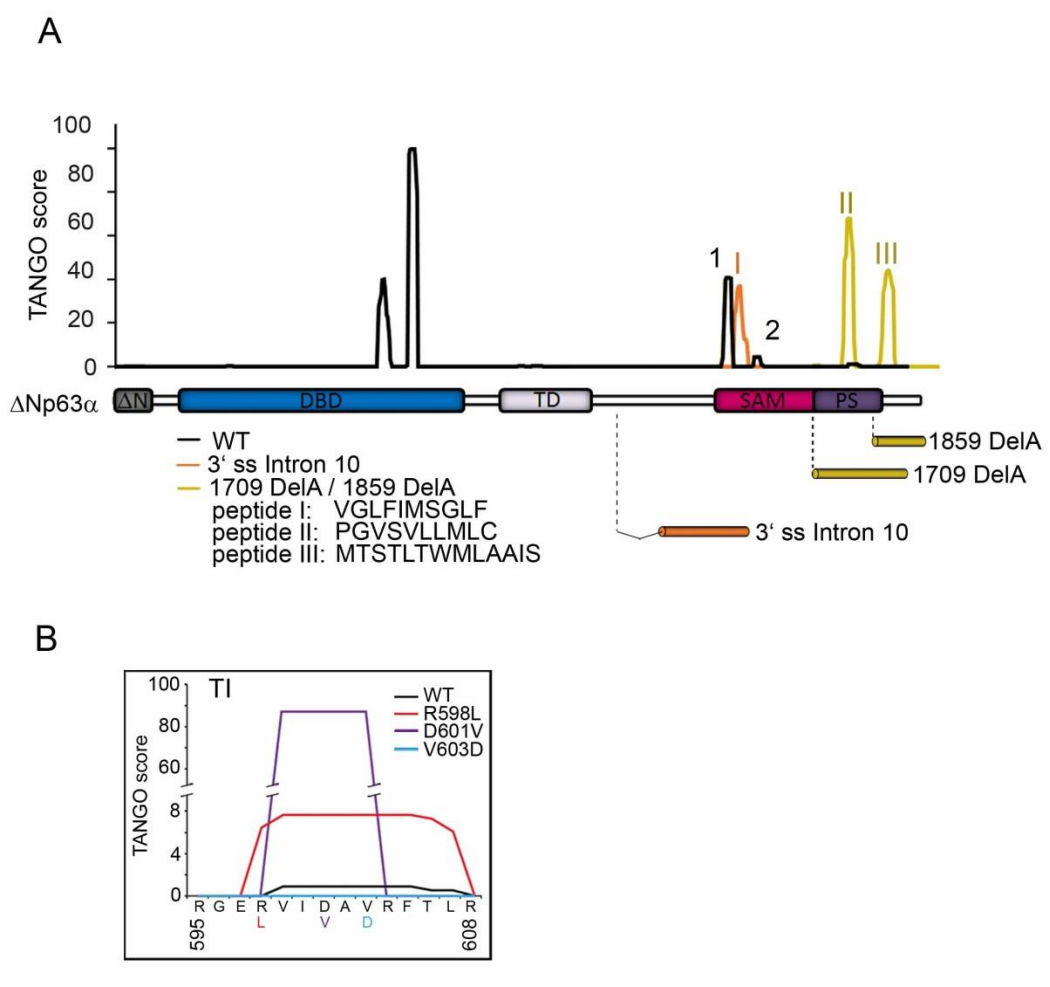

Figure 18. Aggregation propensity of wild type p63 and AEC-associated p63 mutants. A) Grafic representation of the aggregation propensity regions (APRs) predicted by TANGO algorithm in wild type ΔNp63α (in black) and in the presence of the indicated AEC mutations 3'ss intron 10 (in orange) 1709delA and 1859delA (in yellow). B) Detail of APRs in the TI domain of p63 wild type (in black) and in the presence of AEC missense mutations R598L (in red) and D601V (in violet). The V603D variant (in blue) is predicted to abolish the intrinsic aggregation propensity of the TI domain.

Subsequently, together with our collaborators, we identified amino acid substitutions or deletions that were predicted to reduce AEC mutants aggregation propensity using TANGO algorithm. We transfected AEC mutants carrying the mutations that were found to alleviate aggregation in H1299 cells and then we

analyzed the native lysates by BN-PAGE followed by Western blot for p63. Consistently with TANGO prediction, for the L514F mutant, aggregation was alleviated by the introduction of multiple amino acid substitutions in combinations (V603D/V511D/T533D). Single substitutions were also tested but they failed to prevent L514F mutant aggregation (Fig.19A). For 3'ss-int10, 1709delA and 1859delA mutants aggregation was abolished by the deletion of APRs generated by the frameshift mutations (Fig.18A, Fig.19B). Finally, the introduction of the V603D substitution in the TI domain inhibited the aggregation of R598L and D601V mutants (Fig.19C).

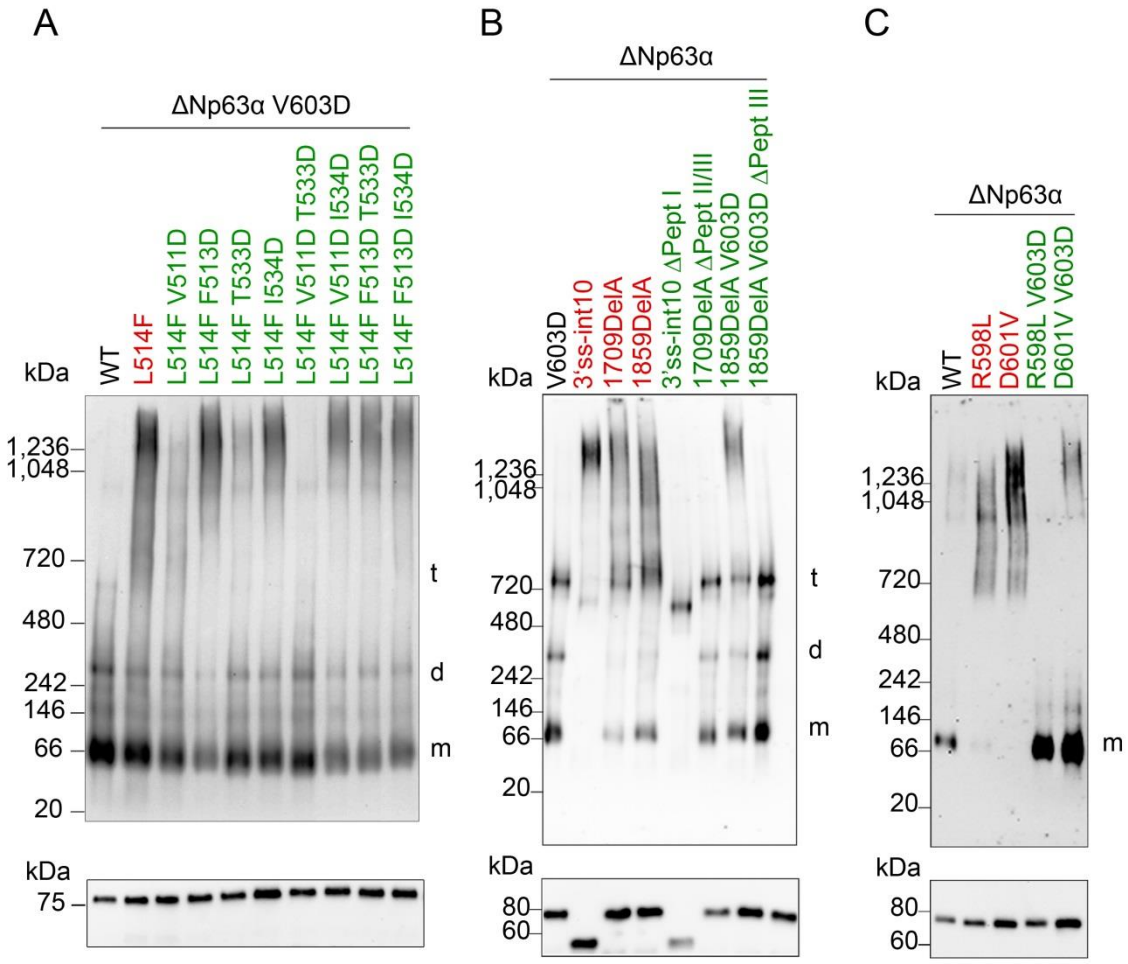

Figure 19. Aggregates formation of AEC-associated p63 mutant proteins with or without mutations or deletions predicted to reduce their aggregation propensity. BN-PAGE (upper) and SDS-PAGE (lower) followed by Western blot for p63 on native

lysates of H1299 cells transfected with wild type p63 or the indicated AEC-associated p63 mutants (in red) or the AEC mutants carrying mutations or deletions that were predicted to prevent their aggregation by TANGO (in green).

To verify whether the impaired transcription function observed in AEC-associated p63 mutants was uniquely associated to protein aggregation, we tested the ability to transactivate KRT14 promoter of the not-aggregating AEC mutant variants, described above, compared to the corresponding AEC mutants, by performing a luciferase reporter assay in HEK293T cells. Data indicated that the L514F mutant bearing the triple substitution V603D/V511D/T533D displayed a restored transactivation activity compared to L514F mutant (Fig.20A). Similarly, the activities of 1709DelA and 1859DelA frameshift mutants were fully restored upon deletion of APRs in the elongated portion of the mutant proteins (Fig.20B). Finally, V603D substitution in R598L and D601V mutants preventing aggregation rescued also mutant p63 ability to transactivate (Fig.20C). Interestingly, V603D substitution alone, predicted to reduce the intrinsic aggregation propensity of the TI domain, retained wild type transcriptional functions (Fig.20A-C).

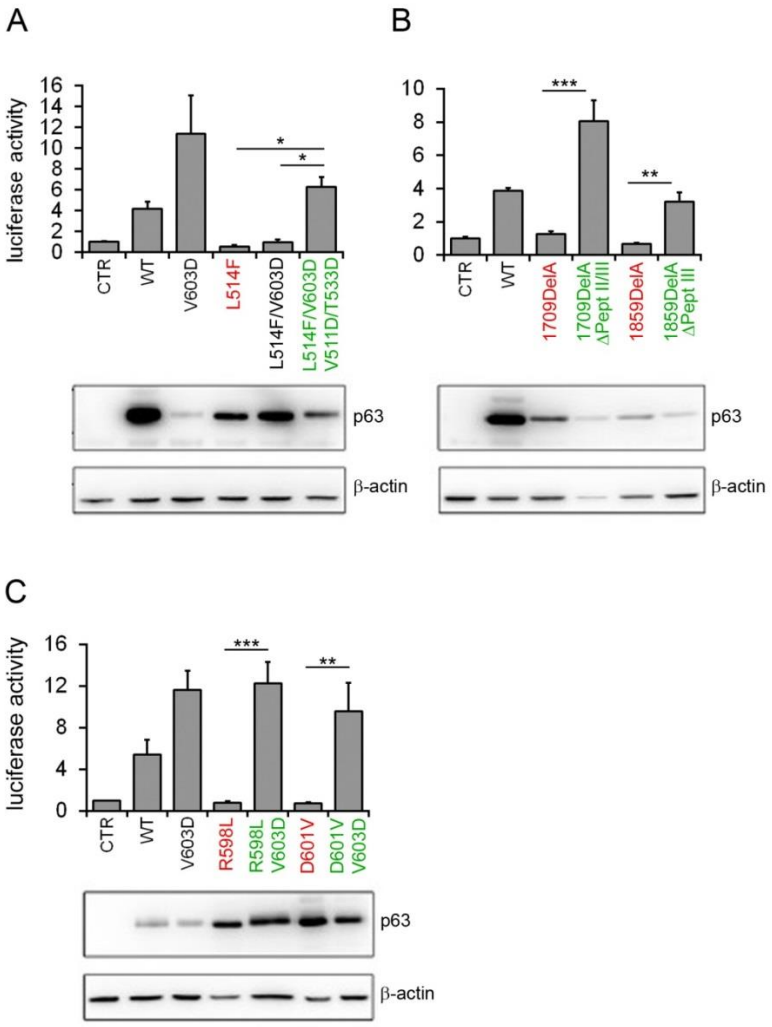

Figure 20. Transactivation activity of AEC-associated p63 mutants with or without mutations or deletions that prevent their aggregation. (A-C) Luciferase reporter assay in HEK293T cells co-transfected with wild type p63 or AEC-associated p63 mutants (in red) or not-aggregating AEC mutant variants (in green) and the K14 promoter-luc vector at a ratio 3:1. A *Renilla* luciferase control vector was co-transfected. Data were normalized for *Renilla* luciferase activity (n=3) (Upper). SDS-PAGE (Lower) followed by Western blot for p63 are shown as control. β-actin was used as loading control. Data are shown as mean of independent samples ± standard error of the mean (SEM). Statistical significance was assessed using one-way ANOVA analysis. * $p \leq 0.05$; ** $p \leq 0.001$; ***$p \leq 0.0001$.

To test the transcriptional activity of not-aggregating AEC mutant variants in a more physiological context, we resorted to a recently developed protocol to convert human dermal fibroblasts (HDFs) into induced keratinocyte-like cells (iKCs) by co-expression of ΔNp63α and the reprogramming factor Krüppel-like factor 4 (KLF4) (Chen et al., 2014). More specifically, we tested the ability of wild type p63, AEC mutants or not-aggregating AEC mutant variants to induce the expression of keratinocyte-specific p63 target genes, namely KRT14 and IRF6, thus leading to the conversion. HDFs were co-infected with retroviruses carrying wild type or mutant p63 and KLF4 and collected after eighteen days, required for the conversion into iKCs, for real time RT-PCR and Western blot analysis. In the presence of wild type p63 or V603D mutant, HDFs were converted into iKCs with the expression of KRT14 and IRF6 genes, measured as mRNA (Fig.21A) and protein (Fig.21B) levels. Consistently with previous observations, AEC mutants L514F, R598L and 1709DelA were unable to induce KRT14 and IRF6 expression and achieve the conversion. Interestingly, deleting the aggregation-prone peptides of the 1709DelA mutant or introducing V603D substitution into the R598L mutant fully rescued their ability to induce expression of KRT14 and IRF6 in HDF (Fig.21A,B). Although at lesser extent, alleviating aggregation of the L514F mutant also rescued its ability to convert HDF to iKC (Fig.21B).

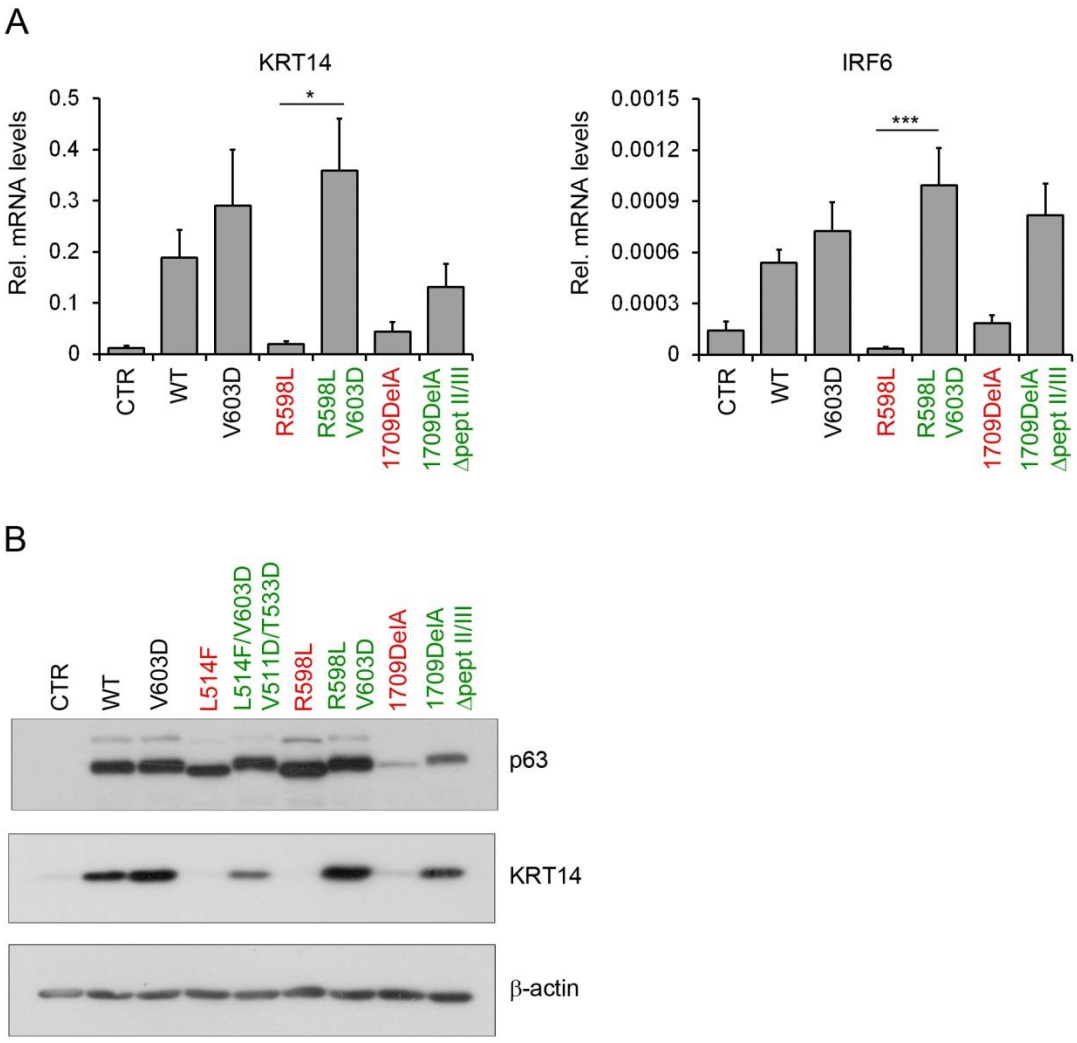

Figure 21. HDF-to-iKC conversion assay in the presence of wild type p63 or AEC-associated p63 mutants with or without mutations or deletions that prevent their aggregation. A) Real-time RT-PCR of keratinocyte-specific p63 target genes (KRT14 and IRF6) in HDFs converted to iKCs by co-infection with retroviruses carrying KLF4 reprogramming factor gene and the indicated p63 mutants. B) Western blot of KRT14 and p63 in iKCs. β-actin was used as loading control. Data are shown as mean ± SEM and statistical significance was assessed using one-way ANOVA analysis. *P ≤ 0.05; **P ≤ 0.001; ***P ≤ 0.0001.

To further investigate the effects of not-aggregating AEC mutant variants in a keratinocyte physiological context, we measured the expression levels of Krt8

gene, repressed by wild type p63, in mouse primary keratinocytes infected with retroviruses carrying wild type p63, the AEC mutants L514F or R598L or the corresponding not-aggregating variants L514F/V603D/V511D/T533P or R598L/V603D, respectively. We collected the native lysates of keratinocytes to check for p63 aggregation by performing BN-PAGE followed by Western blot analysis and isolated RNA samples to measure Krt8 mRNA levels. We found that keratinocytes infected with L514F or R598L mutants displayed p63 aggregation (Fig.22A) and concomitant induction of Krt8 expression, as measured in both RNA (Fig.22B) and protein (Fig.22C) samples. Conversely, p63 aggregation and Krt8 expression were suppressed in the presence of wild type p63 or not-aggregating AEC mutant variants L514FV603D/V511D/T533D and R598L/V603D (Fig.22A-C).

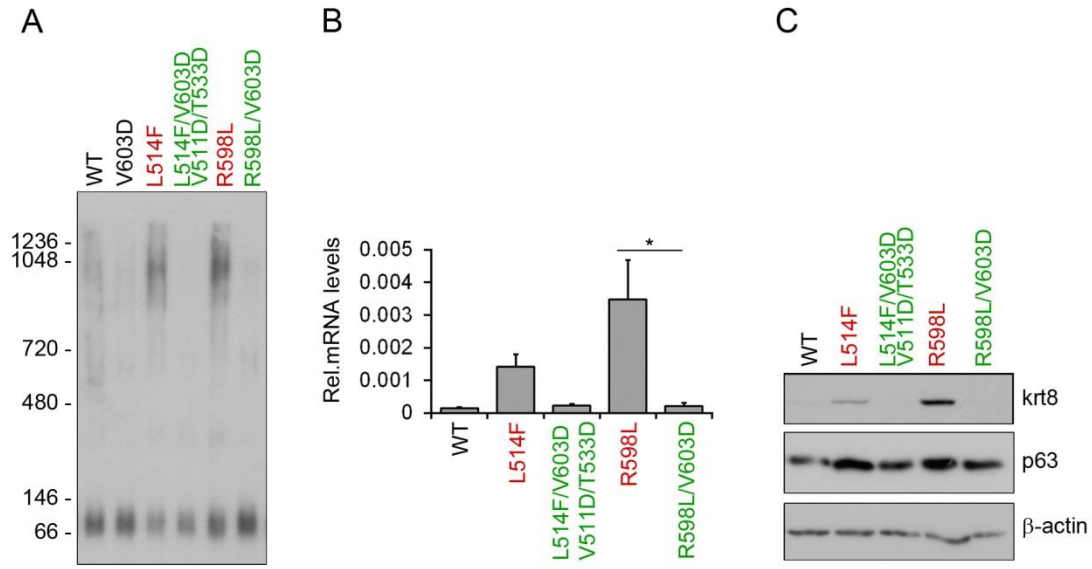

Figure 22. Aggregation and transcriptional activity of AEC-associated p63 mutants with or without mutations predicted to reduce their aggregation propensity in mouse primary keratinocytes. A) BN-PAGE followed by Western blot for p63 in mouse primary keratinocytes infected with retrovirus carrying wild type p63 or the indicated p63 mutants. B) Real time RT-PCR of Krt8 (n=4) and C) Western blot for Krt8 and p63 (lower panel) in mouse primary keratinocytes infected as in A. β-actin was used as loading

control. Data are shown as mean ± SEM and statistical significance was assessed using one-way ANOVA analysis. * $p \leq 0.05$.

Taken together, these results indicated that AEC-associated p63 mutations cause an increased tendency to aggregate and the aggregation is responsible of the impaired transactivation activity of p63. Preventing aggregation rescued AEC mutant transcriptional functions.

4.5 AEC mutant aggregates do not induce Unfolded Protein Response

We next investigated the consequences of the AEC mutant protein aggregates for cellular homeostasis. More specifically, we evaluated whether the accumulation of AEC-associated mutants could elicit endoplasmic reticulum stress, leading to the activation of the Unfolded Protein Response of the Endoplasmic Reticulum (UPR^{ER}). To this aim we measured the activation of some crucial mediators of UPR^{ER} pathways in primary keratinocytes derived from K14-Cre; $p63^{L514Fflox/L514Fflox}$ homozygous mice (L/L) compared to wild type controls (CTR). As positive control of UPR^{ER} activation, we used wild type mouse primary keratinocytes treated with thapsigargin 1 μM, a Ca2+-ATPase inhibitor that leads to ER Ca2+ depletion inducing ER stress. More specifically, we assessed PERK phosphorylation, which is induced upon PERK activation, and the downstream effectors P-eIF2α, eIF2α, ATF4 and Chop in keratinocyte lysates by performing an SDS-PAGE followed by Western blot analysis (Fig.23). We observed that thapsigargin 1μM induced phospho-PERK and ATF4 expression after 1 hour of treatment, whereas Chop

expression was induced after 4 hours of treatment, thus indicating that an UPR^{ER} activation occurred, as expected. On the other hand, none of the tested UPR^{ER}-mediators was induced in L/L keratinocytes compared to CTR, suggesting that AEC mutant p63 accumulation did not cause an UPR^{ER} activation.

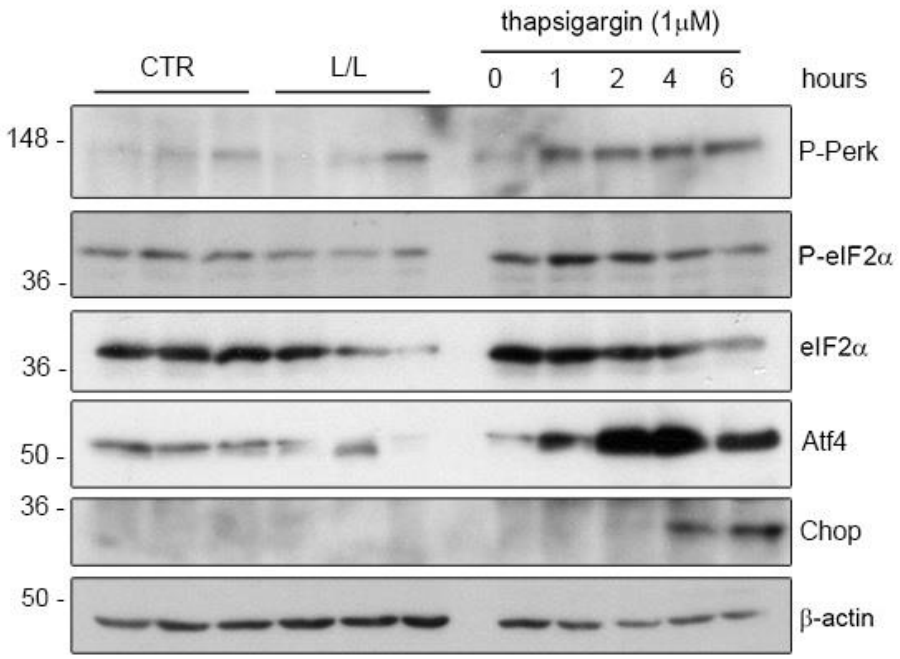

Figure 23. Modulation of UPR^{ER} signaling mediators in the presence of wild type or AEC mutant p63 in mouse primary keratinocytes. SDS-PAGE followed by Western blot in primary keratinocytes derived from p63floxL514F/floxL514F (CTR) or K14-Cre; p63floxL514F/floxL514F (L/L) mice for the following UPR^{ER} mediators: phosphorylated-Perk (P-Perk), phosphorylated-eIF2α (P-eIF2α), eIF2α, Atf4 and Chop. Wild type mouse primary keratinocytes treated with thapsigargin 1μM at different time points were used as positive controls of UPR^{ER} activation.

4.6 AEC-associated p63 mutants interact with specific molecular chaperones involved in protein disaggregation

To identify the proteostasis network involved in the cellular handling of AEC mutant aggregates, we focused on the molecular chaperones specifically recruited to AEC-associated p63 mutants to preserve protein homeostasis. We firstly verified the protein interaction of HSP70, a well-known molecular chaperone involved in many functions of the protein quality control (PQC) system, with wild type or mutant p63. We transfected wild type p63, AEC mutants L514F or R598L or EEC mutant R304Q in H1299 cells and performed an immunoprecipitation experiment using anti-HSP70 antibody. Then, we assessed p63 protein interaction with endogenous HSP70 by analyzing immunoprecipitated (IP) and total (Input) fractions by SDS-PAGE followed by Western blot for p63 and HSP70. As shown in input fractions, the expression levels of endogenous HSP70 remained unvaried upon expression of wild type or mutant p63 proteins. However, HSP70 displayed a strongly increased interaction with L514F and R598L AEC mutants and, to a lesser extent, with R304Q EEC mutant compared to wild type p63 (Fig.24).

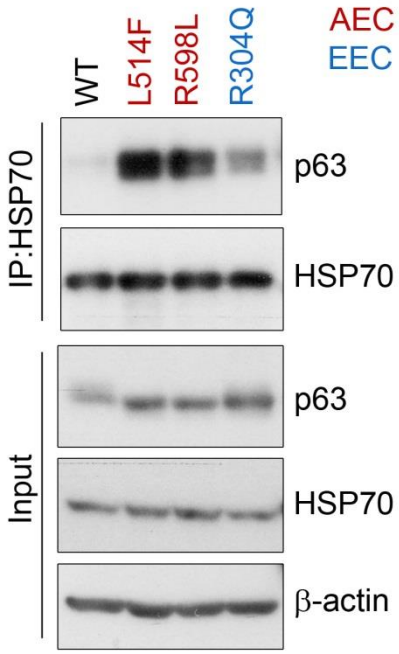

Figure 24. Protein interaction of endogenous HSP70 chaperone with wild type p63, EEC-associated or AEC-associated p63 mutants. Co-immunoprecipitation between endogenous HSP70 and wild type or mutant p63 transfected in H1299 cells. 2.5 mg of total protein were immunoprecipitated using HSP 70/HSC 70 (W27) monoclonal antibody. Immunoprecipitated fraction (IP) was analyzed by SDS-PAGE and Western blot for HSP70 and p63. β-actin was used as loading control. Input fraction is shown as control of HSP70 and p63 expression in the total lysate.

HSP70 is involved in multiple biological processes ranging from protein folding to degradation and can act in the nucleus or in the cytoplasm. Therefore, to further characterize HSP70 interaction with AEC mutants, we firstly investigated whether aggregation occurred in the cytoplasm, where HSP70 could interact with p63 mutant proteins in the attempt to assist their folding, or in the nucleus, where p63 translocates to perform its functions. To this aim, we isolated nuclear and cytoplasmic extracts of keratinocytes derived from K14-Cre; $p63^{+/floxL514F}$, K14-Cre;

p63$^{floxL514F/floxL514F}$ and control mice (p63$^{+/floxL514F}$) and we analyzed them by SDS-PAGE and Western blot for p63, to verify the cellular localization of wild type and mutant p63, and for HSP70 to assess whether the molecular chaperone could be recruited to the mutant protein and co-localize. Both wild type and mutant p63 localized in the nucleus, whereas HSP70 distribution between nucleus and cytoplasm remained unvaried in the presence of p63 mutant protein, compared to the control, indicating that AEC mutants translocated into the nucleus where they formed large aggregates and were likely to interact with nuclear HSP70 (Fig.25).

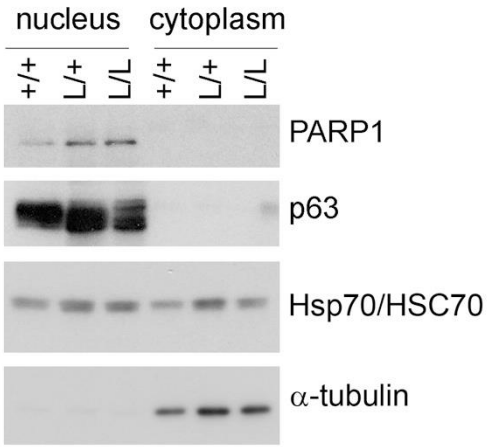

Figure 25. Nuclear/cytoplasmic localization of wild type p63, p63L514F mutant and HSP70 in mouse primary keratinocytes. SDS-PAGE followed by Western blot for p63 and HSP70 on nuclear and cytoplasmic extracts of primary keratinocytes derived from p63$^{+/floxL514F}$ (+/+), K14-Cre; p63$^{+/floxL514F}$ (+/L) and K14-Cre; p63$^{floxL514F/floxL514F}$ (L/L) mice. PARP1 and α-tubulin were used as nuclear and cytoplasmic markers, respectively.

Among the other functions, HSP70 chaperone exhibits a disaggregation activity often supported by a cooperation with DNAJ-proteins. However, some DNAJ proteins can work independently from HSP70 and display anti-aggregation

properties, as discussed in the “Introduction” section. For this reason we tested the protein interaction of wild type and L514F mutant p63 with B-type DNAJ proteins that, as previously demonstrated (Hageman et al., 2010), are able to suppress protein aggregation, namely DNAJB1 and DNAJB6. The last one can be found into two isoforms: the longer DNAJB6a, acting in the nucleus, and the shorter DNAJB6b, acting in both nucleus and cytoplasm. FLAG-tagged wild type or L514F AEC mutant p63 were co-transfected with V5-tagged DNAJB1, DNAJB6a or DNAJB6b in HEK293T cells. Then, FLAG-tagged p63 was immunoprecipitated using anti-FLAG agarose beads and IP and Input fractions were analyzed by SDS-PAGE followed by Western blot analysis for FLAG and V5 tags. DNAJB1 did not exhibit protein interaction either with wild type or with mutant p63. Interestingly, DNAJB6a displayed a stronger interaction with L514F mutant than with wild type p63 (Fig.26A), whereas DNAJB6b interacts exclusively with L514F mutant p63 (Fig.26B).

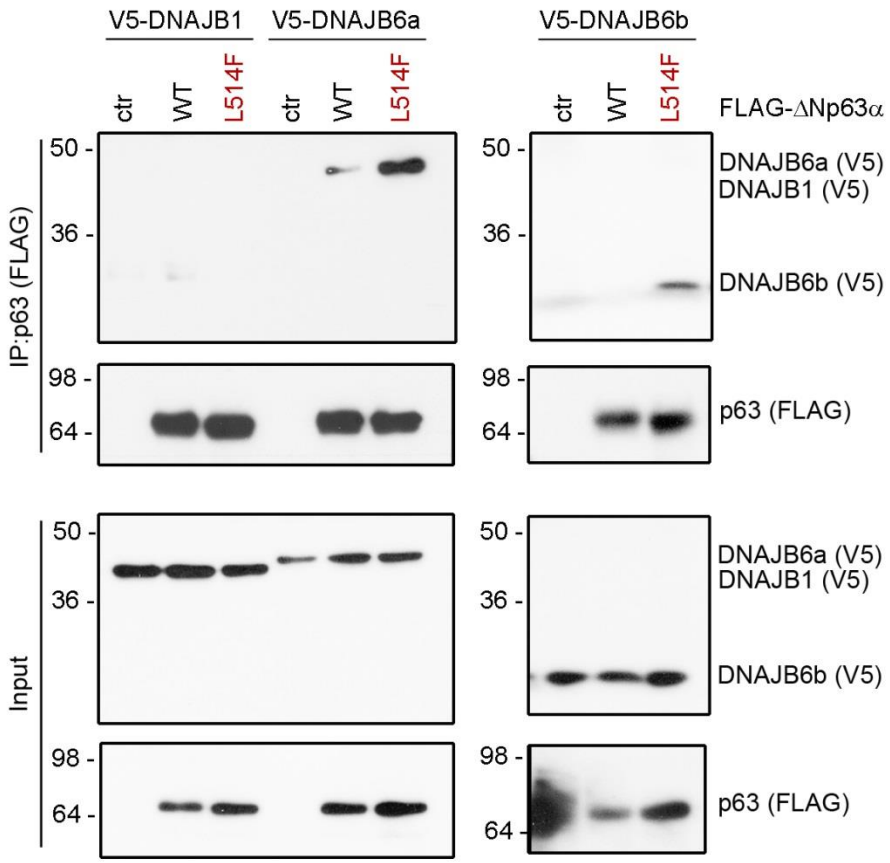

Figure 26. Protein interaction between wild type p63 or p63L514F mutant and DNAJ proteins. A) Co-immunoprecipitation between FLAG-tagged wild type or mutant p63 and V5-tagged DNAJB1 or DNAJB6a co-transfected in HEK293T cells. B) Co-immunoprecipitation between FLAG-tagged wild type or mutant p63 and V5-tagged DNAJB6b co-transfected in HEK293T cells. 3 mg of total protein were immunoprecipitated using anti-FLAGM2 agarose beads (Sigma-Aldrich). Immunoprecipitated (IP) fraction was analyzed by SDS-PAGE and Western blot for FLAG and V5 tags. Input fraction is shown as control of exogenous DNAJs and p63 expression in the total lysate.

Taken together these data indicated that AEC mutants are bound by molecular chaperones involved in disaggregation functions but they elude the activity of PQC system in preventing or suppressing protein aggregation.

4.7 PRIMA-1-Met rescues the morphology of differentiated epidermal keratinocytes derived from an AEC patient

The preliminary data shown above open new avenues to counteract aggregation and hopefully to rescue the skin defects in AEC syndrome, based on targeting the molecular chaperones that specifically interact with AEC mutants to potentiate their anti-aggregation activity.

Alternatively, the proteostasis network can be enhanced using small molecules that bind to mutant proteins and assist the correct folding, acting as “pharmacological chaperones” (Powers et al., 2009). As a first attempt, we recently tested the effect of the small compounds APR-246 (also known as PRIMA-1-Met) and STIMA-1 on AEC mutant p63 functions. PRIMA-1-Met (p53-dependent reactivation and induction of massive apoptosis) is able to restore mutant p53 apoptotic functions in human cancer cells (Bykov et al., 2002) and it has been demonstrated to rescue the epidermal differentiation of skin keratinocytes derived from EEC patients (Shen et al., 2013), targeting EEC-associated mutant p63. STIMA-1 is a low molecular weight compound that reactivates mutant p53 in human tumor cells by stimulating its binding to the DNA (Zache et al., 2008).

Based on the structural homology between p53 and p63, we evaluated the effects of the treatment with PRIMA-1-Met and STIMA-1, used separately or in combination, on human keratinocytes derived from an AEC patient carrying the p63 mutation T537P. In a preliminary screening, we tested the ability of AEC keratinocytes to undergo epidermal differentiation *in vitro* in the presence or in the absence of the small compounds. We previously observed that normal human epidermal keratinocytes (NHEK), but not AEC keratinocytes, were successfully induced to differentiate *in vitro* by high cellular confluence and high calcium

conditions. Keratinocytes were grown in Epilife medium containing Human Keratinocyte Growth Supplement (HKGS) until they reached 100% confluence. Then, the growth medium was switched to Epilife medium supplemented with HKGS and 1.5mM $CaCl_2$ and cells were left to differentiate for 3, 5, 7 and 10 days. During the *in vitro* differentiation process, normal human epidermal keratinocytes enlarged, established closed cell-cell contacts and became flattened, largely recapitulating the differentiation steps of epidermal layers *in vivo* (Fig.27A). On the other hand, AEC keratinocytes displayed an impaired epidermal differentiation *in vitro*, as they largely retained the round shape characteristic of proliferating undifferentiated keratinocytes and, over the days of differentiation, they partially lost cell-cell connections acquiring an elongated morphology (Fig.27B).

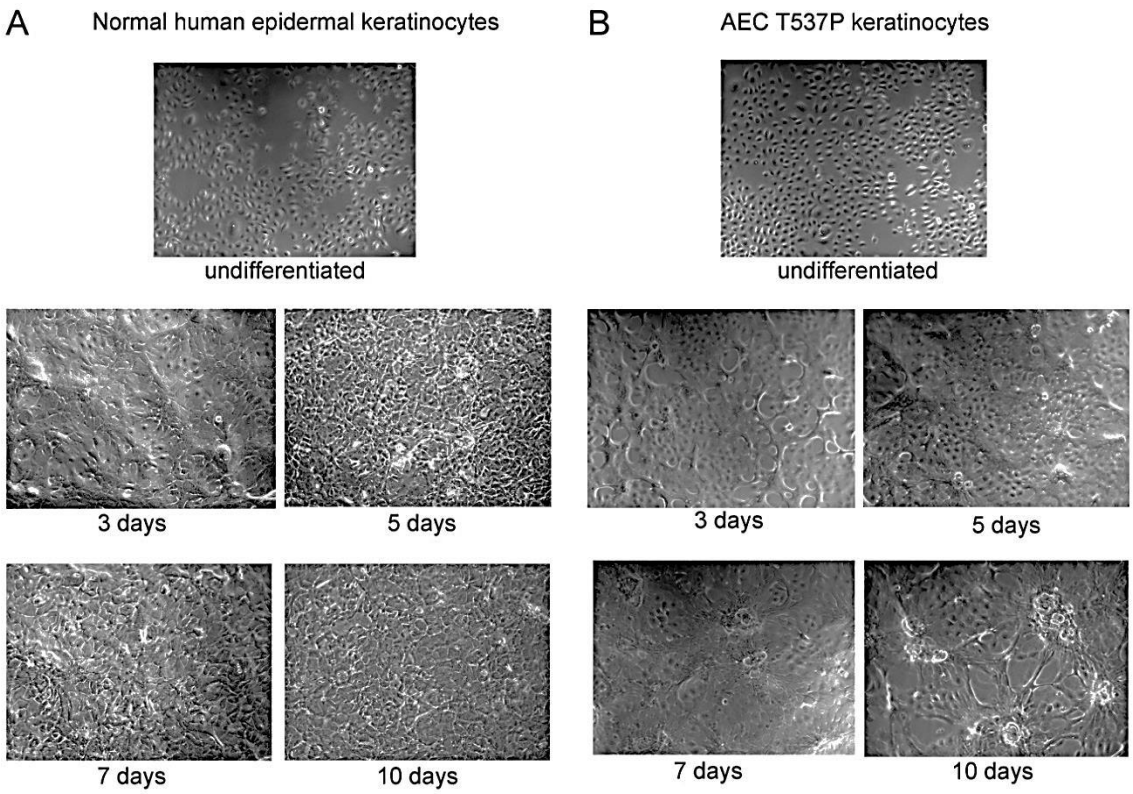

Figure 27. Morphology of normal human epidermal keratinocytes or AEC human keratinocytes undifferentiated and after 3, 5, 7 and 10 days of differentiation. Representative fields acquired using 10X magnification of normal human epidermal keratinocytes (A) and human keratinocytes derived from an AEC patient carrying the p63

mutation T537P (AEC T537P keratinocytes) (B). The epidermal differentiation process of keratinocytes started when cells became 100% confluent and was sustained by the addition of 1.5mM $CaCl_2$ to the growth medium. Pictures were taken 3, 5, 7 and 10 days later.

Therefore, we assessed whether PRIMA-1-Met and/or STIMA-1 treatment could rescue the differentiated morphology of AEC keratinocytes. We treated also normal human epidermal keratinocytes with the compounds as control, to verify if the treatment could interfere with the differentiation process of wild type keratinocytes. Subconfluent keratinocytes were treated with PRIMA-1-Met 30 μM and STIMA-1 10 μM, separately or in combination. After 48 hours, they reached 100% confluence and the differentiation process was induced and sustained by the addition of 1.5 mM $CaCl_2$ to the growth medium. The differentiation process was carried on for 10 days in the presence or in the absence ("not treated") of the compounds. The morphology of differentiated normal human epidermal keratinocytes was not altered by the treatment with PRIMA-1-Met and/or STIMA-1 compared to the not treated cells and no toxic effects were detected using the tested concentrations (Fig.28A). Interestingly, AEC keratinocytes dramatically changed their morphology upon treatment with PRIMA-1-Met compared to the not treated cells, forming a monolayer of enlarged and flatten cells similar to differentiated normal keratinocytes. Conversely, STIMA-1 worsened the morphology AEC keratinocytes, increasing the cell-cell detachment and leaving large holes in the dish. Combined PRIMA-1-Met and STIMA-1 treatment caused a sum of the effects derived from the single treatments, with cells enlargement and flattening and, at the same time, the formation of large holes in the dish (Fig.28B).

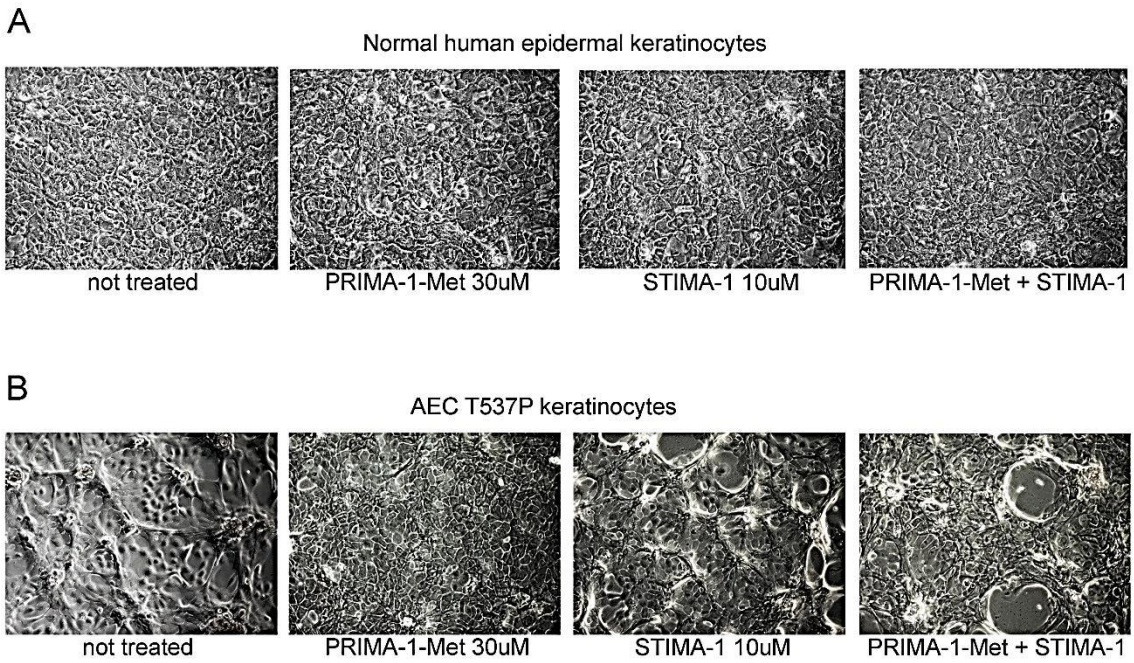

Figure 28. Morphology of differentiated normal human epidermal keratinocytes or AEC human keratinocytes upon treatment with PRIMA-1-Met and/or STIMA-1. Representative fields acquired using 10X magnification of normal human epidermal keratinocytes (NHEK) (A) and human keratinocytes derived from an AEC patient carrying the p63 mutation T537P (B). Subconfluent keratinocytes were treated or not with PRIMA-1-Met 30μM and/or STIMA-1 10μM. After 48 hours they became 100% confluent, the Epilife growth medium was switched to Epilife medium supplied with 1.5 mM $CaCl_2$ and PRIMA-1-Met and STIMA-1 compounds and the differentiation process started. The growth medium was replaced every two days with fresh medium containing $CaCl_2$ and the compounds. Pictures were taken 10 days later.

These preliminary data indicate that PRIMA-1-Met rescued the differentiated morphology of AEC keratinocytes and, together with the previously published effects on mutants p53 and p63, encourage further investigation on structural and functional consequences of this small molecule on AEC-associated mutant p63.

5. DISCUSSION

AEC syndrome is a rare autosomal dominant disorder caused by mutations in the TP63 gene. The severe skin fragility and extensive erosions represent distinctive signs of this p63-associated disorder. The skin lesions can be often life-threatening and require an effective and targeted therapy that, to date, has not been found due also to the poor understanding of the molecular mechanisms underlying the disorder. Here we investigated the structural and functional consequences of p63 mutations causative of AEC syndrome, focusing on the implications for the p63 transcriptional activity on skin-specific target genes.

We found that AEC-associated p63 mutants display an impaired transactivation activity, similarly to the EEC-associated R304Q mutant which is unable to bind to DNA, as previously reported (Celli et al., 1999). We observed also that AEC mutations cause a reduced DNA binding ability of p63, although, differently from EEC-associated mutations, they do not affect directly the DNA binding domain of the protein. Importantly, using a p53-p63 DNA binding competition assay we demonstrated that AEC mutants were able to interfere with p53 binding to DNA at increased doses compared to p63 wild type, whereas the EEC R304Q mutant did not compete with p53 at any tested concentration. These results indicate that DNA binding impairment is not an intrinsic property of the AEC mutants as is the case for EEC mutants, but rather an indirect consequence of structural aberrations in the protein, specifically caused by the AEC-associated mutations, which lead to a reduced p63 affinity for DNA. Interestingly, we found that two tested SHFM-associated mutations falling in the carboxyl-terminal domain of p63 did not impair either DNA binding or transactivation activity of p63, thus indicating that they interfere with p63 functions by different mechanisms.

These findings underline the close genotype-to-phenotype correlation which characterizes p63 syndromes. Despite the wide variety of p63 mutations associated to AEC syndrome, we found that all of them lead to conformational changes in p63 protein with the exposure of hydrophobic residues with a high aggregation propensity. AEC mutations can cause aggregation by either aberrant protein elongation introducing aggregation-prone peptides (e.g., 3'ss intron 10, 1709DelA, 1859DelA), enhancing the intrinsic low aggregating-prone region (APR) of the TI domain (e.g., R598L, D601V) or by conformational changes that expose peptides with a natural high aggregation propensity (e.g., L514F). These evidences emerged at the first from the TANGO analysis of the predicted APRs in AEC mutant p63 proteins and then were confirmed also in cells. Importantly, we assessed that p63 aggregation occurs in human keratinocytes derived by an AEC patient. Furthermore, we have showed that p63 protein aggregation occurs in mammalian cells overexpressing AEC mutants as well as in primary keratinocytes derived from a newly developed conditional knock-in mouse model for AEC syndrome ($p63^{+/floxL514F}$), recently generated in our laboratory, in which the L514F AEC mutation was expressed only in the presence of Cre recombinase. We induced the p63L514F expression *in vitro*, by infection of keratinocytes with adeno-Cre, or used keratinocytes isolated from mice which expressed p63L514F mutant in the skin (K14Cre; $p63^{+/floxL514F}$), as they carried the Cre recombinase gene under the control of the K14 promoter. Our conditional knock-in AEC mouse model (K14Cre; $p63^{floxL514F/floxL514F}$) fully recapitulates the skin defects and erosions found in AEC patients and allows to study the evolution of the skin phenotype in the adult avoiding cleft palate, another hallmark of AEC phenotype, which caused neonatal lethality in AEC constitutive knock-in mice (Ferone et al., 2012). We found that the expression levels of keratinocyte-specific p63 target genes, involved in the development and the differentiation of the skin, were reduced in AEC mouse

keratinocytes compared to wild type controls. Interestingly, some genes that are known to be negatively regulated by p63 (e.g., Smad7, Krt8) are induced in the presence of p63L514F mutant, thus indicating that protein aggregation impaired both transactivating and repressing functions of p63.

Of great relevance, we found that p63 transcriptional activity can be rescued by preventing aggregation upon deletion of aggregating peptides or introduction of specific amino acid substitutions that reduce the aggregation propensity of AEC mutants. These findings were confirmed in multiple assays and cellular systems and strengthen the idea that the impaired transcriptional functions of p63 and, consequentially, the fragile skin phenotype were uniquely caused in AEC syndrome by protein aggregation.

In a second part of the work, we investigated the effects of p63 aggregates on protein homeostasis. The Protein Quality Control (PQC) system responds to protein aggregation by different mechanisms to target aggregating proteins and assist their disaggregation. These mechanisms often involve the HSP70 molecular chaperone, which is provided of a standalone disaggregase activity supported by specific co-chaperones (Kampinga et al., 2010; Nillegoda et al., 2017). However, protein aggregates can also trap crucial components of the proteostasis network, which are rendered not available, thus leading to a reduced proteostasis capacity (Hipp et al., 2014). We observed that AEC-associated mutants and, to a lesser extent, EEC-mutant R304Q but not wild type p63 interact with endogenous HSP70, when overexpressed in H1299 cells. Interestingly, the expression levels of endogenous HSP70 remained unchanged upon expression of mutant or wild type p63, indicating that HSP70 is not upregulated in the presence of p63 mutant proteins, but it strongly interacts with aggregating- AEC mutants. Furthermore, we verified whether aggregation could compromise nucleocytoplasmic shuttling of

p63, evaluating also if HSP70 is recruited in the same compartment of the mutant protein. The analysis of nuclear and cytoplasmic extracts of keratinocytes derived from AEC mice revealed that mutant p63 localizes in the nucleus whereas HSP70 is detectable in both nucleus and cytoplasm and its distribution between the two compartments is not altered in mutant keratinocytes compared to wild type controls. In addition, we assessed that AEC mutant p63 did not induce ER stress nor the activation of the Unfolded Protein Response of the Endoplasmic Reticulum (UPR^{ER}), thus suggesting that misfolded p63 mutant protein is not retained in the ER, but it translocates to the nucleus where it forms protein aggregates and interacts with nuclear HSP70. The interaction between HSP70 and aggregating AEC mutants opens to different interpretations. HSP70 could be recruited at the p63 aggregate surface, but it fails to execute protein disaggregation. On the other hand, HSP70 could be non-specifically trapped in p63 aggregates, therefore the chaperone availability could be reduced favoring further enrichment of aggregating-prone mutant p63 or possibly other proteins in the nucleus. However, a strengthened proteostasis machinery is required to eventually assist the correct folding of AEC mutant p63 and prevent protein aggregation. More specifically, our goal has been to identify molecular chaperones or co-chaperones, specifically interacting with AEC mutants, whose activity could be enhanced to promote a targeted effect on p63.

The multifunctionality of HSP70 is often driven by DNAJ proteins co-chaperones, which deliver specific unfolded client proteins to HSP70 stimulating also its ATPase activity (Kampinga et al., 2010). In addition, a subclass of the DNAJB family, particularly DNAJB6a, DNAB6b and DNAJB8, can display also anti-aggregating HSP70-independent functions (Hageman et al., 2010). Interestingly, we found that AEC mutant L514F, and not wild type p63, specifically interacts with DNAJB6a and DNAJB6b co-chaperones when co-overexpressed in

HEK293T cells. Importantly, both isoforms DNAJB6a and DNAJB6b act in the nucleus, where p63 aggregates accumulate.

Taken together, these data provide new elements to design a targeted strategy aimed to prevent the aggregation of AEC-associated p63 mutant proteins, by selectively modulating the activity of AEC mutants interactors involved in the PQC system.

Alternatively, a chemical approach could be used to deal with protein aggregation. Previous published studies demonstrated that small molecules were able to assist the correct folding and rescue the function of aggregating-mutant p53 in cancer (Bykov et al., 2002, Zache et al., 2008) or mutant p63 causative of EEC syndrome (Shen et al., 2013, Shalom-Feuerstein et al., 2013). Based on these studies, we tested the effects of PRIMA-1-Met (p53-dependent reactivation and induction of massive apoptosis) and STIMA-1 (SH group-targeting compound that induces massive apoptosis) on epidermal keratinocytes derived from an AEC patient carrying the p63 mutation T537P. We found that AEC keratinocytes displayed an impaired epidermal differentiation *in vitro* compared to normal keratinocytes and this impairment was morphologically rescued by the treatment with PRIMA-1-Met. Conversely, STIMA-1 or the combined PRIMA-1-Met/STIMA-1 treatment caused more dramatic alterations of AEC keratinocytes morphology during differentiation. Therefore, this preliminary screening identifies PRIMA-1-Met as a small molecule potentially acting as a “pharmacological chaperone” for AEC mutant p63 proteins, encouraging to further investigate its effects at structural and molecular levels.

In conclusion, our studies indicate that the AEC syndrome is a protein aggregation disorder and that reverting mutant p63 aggregation leads to a functional rescue. Importantly, our preliminary findings suggest potential

therapeutic approaches to obtain a phenotypical rescue in AEC patients, by increasing the proteostasis efficiency, using “proteostasis modulators”, or by small molecules designed to work as “pharmacological chaperones” for the mutant protein.

6. REFERENCES

Antonini D, Russo MT, De Rosa L, Gorrese M, Del Vecchio L, Missero C. (2010) Transcriptional repression of miR-34 family contributes to p63-mediated cell cycle progression in epidermal cells. J Invest Dermatol 130:1249–1257.

Balchin, D, Hayer-Hartl, M, and Hartl FU. (2016) In vivo aspects of protein folding and quality control. Science 353, aac4354.

Barrow LL, van Bokhoven H, Daack-Hirsch S, Andersen T, van Beersum SE, Gorlin R, Murray JC. (2002) Analysis of the p63 gene in classical EEC syndrome, related syndromes, and non-syndromic orofacial clefts. J Med Genet 39:559-566.

Bykov VJ, Issaeva N, Shilov A, Hultcrantz M, Pugacheva E, Chumakov P, Bergman J, Wiman KG, Selivanova G. (2002) Restoration of the tumor suppressor function to mutant p53 by a low-molecular-weight compound. Nat Med 8:282–288.

Bertola DR, Kim CA, Albano LM, Scheffer H, Meijer R, van Bokhoven H. (2004) Molecular evidence that AEC syndrome and Rapp-Hodgkin syndrome are variable expression of a single genetic disorder. Clin Genet 66:79-80.

Candi E, Rufini A, Terrinoni A, Dinsdale D, Ranalli M, Paradisi A, De Laurenzi V, Spagnoli LG, Catani MV, Ramadan S, Knight RA, Melino G. (2006) Differential roles of p63 isoforms in epidermal development: selective genetic complementation in p63 null mice. Cell Death Differ, 13, pp. 1037-1047

Candi E, Rufini A, Terrinoni A, Giamboi-Miraglia A, Lena AM, Mantovani R, Knight R, Melino G. (2007) DeltaNp63 regulates thymic development through enhanced expression of FgfR2 and Jag2. Proc Natl Acad Sci U S A 104:11999-12004.

Carra, S, Seguin SJ, Lambert, H & Landry, J (2008) HspB8 chaperone activity toward poly(Q)-containing proteins depends on its association with Bag3, a stimulator of macroautophagy. J. Biol. Chem. 283, 1437–1444

Carroll DK, Carroll JS, Leong CO, Cheng F, Brown M, Mills AA, Brugge JS, Ellisen LW. (2006) p63 regulates an adhesion programme and cell survival in epithelial cells. Nat Cell Biol 8:551-561

Celli J, Duijf P, Hamel BC, Bamshad M, Kramer B, Smits AP, Newbury-Ecob R, Hennekam RC, Van Buggenhout G, van Haeringen A, Woods CG, van Essen AJ, de Waal R, Vriend G, Haber DA, Yang A, McKeon F, Brunner HG, van Bokhoven H. (1999) Heterozygous germline mutations in the p53 homolog p63 are the cause of EEC syndrome. Cell 99:143-153.

Chen Y, Mistry DS, Sen GL (2014) Highly rapid and efficient conversion of human fibroblasts to keratinocyte-like cells. J Invest Dermatol 134:335–344.

Chiti F and Dobson CM. (2017) Protein misfolding, amyloid formation, and human disease: a summary of progress over the last decade. Annu. Rev. Biochem. 86, 27–68.

Cicero DO, Falconi M, Candi E, Mele S, Cadot B, Di Venere A, Rufini S, Melino G, Desideri A. (2006) NMR structure of the p63 SAM domain and dynamical properties of G534V and T537P pathological mutants, identified in the AEC syndrome. Cell Biochem Biophys 44:475–489

Coutandin D, Osterburg C, Srivastav RK, Sumyk M, Kehrloesser S, Gebel J, Tuppi M, Hannewald J, Schäfer B, Salah E, Mathea S, Müller-Kuller U, Doutch J, Grez M, Knapp S, Dötsch V. (2016) Quality control in oocytes by p63 is based on a springloaded activation mechanism on the molecular and cellular level. Elife 5:e13909.

Crum CP, McKeon FD (2010) p63 in epithelial survival, germ cell surveillance, and neoplasia. Annu Rev Pathol 5:349–371.

De Rosa L, Antonini D, Ferone G, Russo MT, Yu PB, Han R, Missero C. (2009) p63 Suppresses non-epidermal lineage markers in a bone morphogenetic protein-dependent manner via repression of Smad7. J Biol Chem 284(44):30574-30582.

Deutsch GB, Zielonka EM, Coutandin D, Weber TA, Schäfer B, Hannewald J, Luh LM, Durst FG, Ibrahim M, Hoffmann J, Niesen FH, Sentürk A, Kunkel H, Brutschy B, Schleiff E, Knapp S, Acker-Palmer A, Grez M, McKeon F, Dötsch V. (2011) DNA damage in oocytes induces a switch of the quality control factor TAp63α from dimer to tetramer. Cell 144:566–576.

Duijf PH, Vanmolkot KR, Propping P, Friedl W, Krieger E, McKeon F, Dotsch V, Brunner HG, van Bokhoven H. (2002) Gain-of-function mutation in ADULT syndrome reveals the presence of a second transactivation domain in p63. Hum Mol Genet 11:799-804.

el-Deiry WS, Tokino T, Velculescu VE, Levy DB, Parsons R, Trent JM, Lin D, Mercer WE, Kinzler KW, Vogelstein B. (1993) WAF1, a potential mediator of p53 tumor suppression. *Cell* 75(4):817-825.

Ferone G, Mollo MR, Thomason HA, Antonini D, Zhou H, Ambrosio R, De Rosa L, Salvatore D, Getsios S, van Bokhoven H, Dixon J, Missero C. (2013) p63 control of desmosome gene expression and adhesion is compromised in AEC syndrome. Hum Mol Genet 22:531–543.

Ferone G, Mollo MR, Missero C. (2015) Epidermal cell junctions and their regulation by p63 in health and disease. Cell Tissue Res. 360(3):513-28

Ferone G, Thomason HA, Antonini D, De Rosa L, Hu B, Gemei M, Zhou H, Ambrosio R, Rice DP, Acampora D, van Bokhoven H, Del Vecchio L, Koster MI, Tadini G, Spencer-Dene B, Dixon M, Dixon J, Missero C (2012) Mutant p63 causes defective expansion of ectodermal progenitor cells and impaired FGF signalling in AEC syndrome. EMBO Mol Med. 4(3):192-205.

Frakes AE, Dillin A. (2017) The UPR^{ER}: Sensor and Coordinator of Organismal Homeostasis. Mol Cell. 15;66(6):761-771.

Fuchs E, Green H. (1980) Changes in keratin gene expression during terminal differentiation of the keratinocyte. Cell 19:1033-1042.

Fuchs E. (2007) Scratching the surface of skin development. Nature 445:834-842.

Ghioni P, D'Alessandra Y, Mansueto G, Jaffray E, Hay RT, La Mantia G, Guerrini L. (2005) The protein stability and transcriptional activity of p63alpha are regulated by SUMO-1 conjugation. Cell Cycle 4: 183–190.

Hageman J and Kampinga HH. (2009) Computational analysis of the human HSPH/HSPA/DNAJ family and cloning of a human HSPH/HSPA/DNAJ expression library. Cell Stress Chaperones 14, 1–21

Hageman J, Rujano MA, van Waarde MA, Kakkar V, Dirks RP, Govorukhina N, Oosterveld-Hut HM, Lubsen NH, Kampinga HH. (2010) A DNAJB chaperone subfamily with HDAC-dependent activities suppresses toxic protein aggregation. Mol Cell. 12;37(3):355-69.

Hanai R and Mashima K. (2003) Characterization of two isoforms of a human DnaJ homologue, HSJ2. Mol. Biol. Rep. 30, 149–153.

Harding, H.P., Zhang, Y., and Ron, D. (1999) Protein translation and folding are coupled by an endoplasmic-reticulum-resident kinase. Nature 397, 271–274.

Hartl FU & Hayer-Hartl M. (2009) Converging concepts of protein folding in vitro and in vivo. Nature Struct. Mol. Biol. 16, 574–581.

Hay RJ, Wells RS. (1976) The syndrome of ankyloblepharon, ectodermal defects and cleft lip and palate: an autosomal dominant condition. Br J Dermatol 94:277-289.

Helton ES, Zhu J, Chen X. (2006) The unique NH2-terminally deleted (DeltaN) residues, the PXXP motif, and the PPXY motif are required for the transcriptional activity of the DeltaN variant of p63. J Biol Chem 281:2533-2542.

Hipp MS, Park SH., and Hartl FU. (2014) Proteostasis impairment in protein-misfolding and -aggregation diseases. Trends Cell Biol. 24, 506–514.

Houck SA, Singh S, Cyr DM. (2012) Cellular responses to misfolded proteins and protein aggregates. Methods Mol. Biol. 832:455–61

Howarth JL, Kelly S, Keasey MP, Glover C, Lee YB, Mitrophanous K, Chapple JP, Gallo JM, Cheetham ME, Uney JB. (2007) Hsp40 Molecules That Target to the Ubiquitin-proteasome System Decrease Inclusion Formation in Models of Polyglutamine Disease. Mol Ther. Jun;15(6):1100-1105.

Huelsken J, Vogel R, Erdmann B, Cotsarelis G, Birchmeier W (2001) beta-Catenin controls hair follicle morphogenesis and stem cell differentiation in the skin. Cell 105:533–545

Ianakiev P, Kilpatrick MW, Toudjarska I, Basel D, Beighton P, Tsipouras P. (2000) Split-hand/split-foot malformation is caused by mutations in the p63 gene on 3q27. Am J Hum Genet 67:59–66.

Jeng W, Lee S, Sung N, Lee J, Tsai FT. (2015) Molecular chaperones: guardians of the proteome in normal and disease states. F1000Research 4:1448

Julapalli MR, Scher RK, Sybert VP, Siegfried EC, Bree AF (2009) Dermatologic findings of ankyloblepharon-ectodermal defects-cleft lip/palate (AEC) syndrome. Am J Med Genet A 149A:1900–1906.

Kampinga HH, Craig EA. (2010) The HSP70 chaperone machinery: J proteins as drivers of functional specificity. Nat Rev Mol Cell Biol. Aug;11(8):579-92.

Kantaputra PN, Hamada T, Kumchai T, McGrath JA. (2003) Heterozygous mutation in the SAM domain of p63 underlies Rapp-Hodgkin ectodermal dysplasia. J Dent Res 82:433-437.

Kehrloesser S, Osterburg C, Tuppi M, Schäfer B, Vousden KH, Dötsch V. (2016) Intrinsic aggregation propensity of the p63 and p73 TI domains correlates with p53R175H interaction and suggests further significance of aggregation events in the p53 family. Cell Death Differ 23:1952–1960.

Koster MI, Dai D, Marinari B, Sano Y, Costanzo A, Karin M, Roop DR. (2007) p63 induces key target genes required for epidermal morphogenesis. Proc Natl Acad Sci U S A 104:3255-3260.

Koster MI, Kim S, Mills AA, DeMayo FJ, Roop DR. (2004) p63 is the molecular switch for initiation of an epithelial stratification program. Genes Dev 18: 126–131.

Koster MI, Roop DR. (2004) The role of p63 in development and differentiation of the epidermis. J Dermatol Sci 34:3-9.

Laufen T, Mayer MP, Beisel C, Klostermeier D, Mogk A, Reinstein J, Bukau B. (1999) Mechanism of regulation of Hsp70 chaperones by DnaJ cochaperones. Proc. Natl Acad. Sci. USA 96, 5452–5457

Laurikkala J, Mikkola ML, James M, Tummers M, Mills AA, Thesleff I. (2006) p63 regulates multiple signalling pathways required for ectodermal organogenesis and differentiation. Development 133: 1553-1563.

Marciniak SJ, Yun CY, Oyadomari S, Novoa I, Zhang Y, Jungreis R, Nagata K, Harding HP and Ron D. (2004) CHOP induces death by promoting protein synthesis and oxidation in the stressed endoplasmic reticulum. Genes Dev. 18, 3066–3077.

Mayer MP, and Bukau B. (2005) Hsp70 chaperones: cellular functions and molecular mechanism. Cell. Mol. Life Sci. 62, 670–684.

McCarty JS, Buchberger A, Reinstein J and Bukau B. (1995) The role of ATP in the functional cycle of the DnaK chaperone system. J. Mol. Biol. 249, 126–137

McGrath JA, Duijf PH, Doetsch V, Irvine AD, de Waal R, Vanmolkot KR, Wessagowit V, Kelly A, Atherton DJ, Griffiths WA, Orlow SJ, van Haeringen A, Ausems MG, Yang A, McKeon F, Bamshad MA, Brunner HG, Hamel BC, van Bokhoven H. (2001) Hay-Wells syndrome is caused by heterozygous missense mutations in the SAM domain of p63. Hum Mol Genet. Feb 1;10(3):221-9.

Mills AA, Zheng B, Wang XJ, Vogel H, Roop DR, Bradley A. (1999) p63 is a p53 homologue required for limb and epidermal morphogenesis. Nature 398:708-713.

Mogk A, Bukau B, Kampinga HH. (2018) Cellular Handling of Protein Aggregates by Disaggregation Machines. Mol Cell. Jan 18;69(2):214-226.

Mollo MR, Antonini D, Mitchell K, Fortugno P, Costanzo A, Dixon J, Brancati F, Missero C (2015) p63-dependent and independent mechanisms of nectin-1 and nectin-4 regulation in the epidermis. Exp Dermatol. 24(2):114-9.

Nguyen B1, Lefort K, Mandinova A, Antonini D, Devgan V, Della Gatta G, Koster MI, Zhang Z, Wang J, Tommasi di Vignano A, Kitajewski J, Chiorino G, Roop DR, Missero C, Dotto GP. (2006) Cross-regulation between Notch and p63 in keratinocyte commitment to differentiation. Genes Dev 20(8):1028-1042.

Nillegoda NB, Stank A, Malinverni D, Alberts N, Szlachcic A, Barducci A, De Los Rios P, Wade RC and Bukau B. (2017) Evolution of an intricate J-protein network driving protein disaggregation in eukaryotes. eLife 6, https://doi.org/10.7554/eLife.24560.

Petiot A, Conti FJ, Grose R, Revest JM, Hodivala-Dilke KM, Dickson C. (2003) A crucial role for Fgfr2-IIIb signalling in epidermal development and hair follicle patterning. Development. 130(22): 5493-501.

Powers ET, Morimoto RI, Dillin A, Kelly JW, Balch WE. (2009) Biological and chemical approaches to diseases of proteostasis deficiency. Annu Rev Biochem. 2009;78:959-91.

Qiao F, Bowie JU. (2005) The many faces of SAM. Sci STKE (286):re7.

Ramsey MR, He L, Forster N, Ory B, Ellisen LW. (2011) Physical association of HDAC1 and HDAC2 with p63 mediates transcriptional repression and tumor maintenance in squamous cell carcinoma. Cancer Res 71:4373–4379.

Rice R, Spencer-Dene B, Connor EC, Gritli-Linde A, McMahon AP, Dickson C, Thesleff I, Rice DP. (2004) Disruption of Fgf10/Fgfr2b-coordinated epithelial–mesenchymal interactions causes cleft palate. J Clin Invest 113: 1692-1700.

Rinne T, Bolat E, Meijer R, Scheffer H, van Bokhoven H. (2009) Spectrum of p63 mutations in a selected patient cohort affected with ankyloblepharon-ectodermal defects-cleft lip/palate syndrome (AEC). Am J Med Genet A 149A:1948-1951.

Rinne T, Brunner HG, van Bokhoven H. (2007) p63-associated disorders. Cell Cycle 6:262-268.

Rinne T, Hamel B, van Bokhoven H, Brunner HG. (2006) Pattern of p63 mutations and their phenotypes–Update. Am J Med Genet A 140:1396–1406.

Russo C, Osterburg C, Sirico A, Antonini D, Ambrosio R, Würz JM, Rinnenthal J, Ferniani M, Kehrloesser S, Schäfer B, Güntert P, Sinha S, Dötsch V, Missero C. (2018) Protein aggregation of the p63 transcription factor underlies severe skin fragility in AEC syndrome. Proc Natl Acad Sci USA 115(5):E906-E915

Sathyamurthy A, Freund SM, Johnson CM, Allen MD, Bycroft M. (2011) Structural basis of p63α SAM domain mutants involved in AEC syndrome. FEBS J. 278(15): 2680-8.

Schultz, J., Ponting, C. P., Hofmann, K., and Bork, P. (1997) SAM as a protein interaction domain involved in development regulation. Protein Sci 6: 249–253.

Senoo M, Pinto F, Crum CP, McKeon F. (2007) p63 Is essential for the proliferative potential of stem cells in stratified epithelia. Cell 129:523-536.

Serra-Pages, C., Kedersha, N. L., Fazikas, L., Medley, Q., Debant, A., and Streuli, M. (1995) The LAR transmembrane protein tyrosine phosphatase and a coiled-coil LAR interacting protein co-localize at focal adhesions. EMBO J. 14: 2827–2838.

Schultz, J, Ponting, CP, Hofmann, K, and Bork P. (1997) SAM as a protein interaction domain involved in development regulation. Protein Sci. 6, 249–253.

Serber Z, Lai HC, Yang A, Ou HD, Sigal MS, Kelly AE, Darimont BD, Duijf PH, Van Bokhoven H, McKeon F, Dötsch V. (2002) A C-terminal inhibitory domain controls the activity of p63 by an intramolecular mechanism. Mol Cell Biol 22: 8601–8611.

Shalom-Feuerstein R, Serror L, Aberdam E, Müller FJ, van Bokhoven H, Wiman KG, Zhou H, Aberdam D, Petit I. (2013) Impaired epithelial differentiation of induced pluripotent stem cells from ectodermal dysplasia-related patients is rescued by the small compound APR-246/PRIMA-1MET. Proc Natl Acad Sci U S A. 110(6):2152-6.

Shen J, van den Bogaard EH, Kouwenhoven EN, Bykov VJ, Rinne T, Zhang Q, Tjabringa GS, Gilissen C, van Heeringen SJ, Schalkwijk J, van Bokhoven H, Wiman KG, Zhou H. (2013) APR-246/PRIMA-1(MET) rescues epidermal differentiation in skin keratinocytes derived from EEC syndrome patients with p63 mutations. Proc Natl Acad Sci U S A. 110(6):2157-62.

Simpson CL, Patel DM, Green KJ. (2011) Deconstructing the skin: cytoarchitectural determinants of epidermal morphogenesis. Nat Rev Mol Cell Biol 12:565-580.

Sontag EM, Samant RS, Frydman J. (2017) Mechanisms and Functions of Spatial Protein Quality Control. Annu Rev Biochem. Jun 20;86:97-122.

Stapleton D, Balan I, Pawson Y, and Sicheri F. (1999) The crystal structure of an Eph receptor SAM domain reveals a mechanism for modular dimerization. Nat. Struct. Biol. 6: 44–49.

Straub WE, Weber TA, Schäfer B, Candi E, Durst F, Ou HD, Rajalingam K, Melino G, Dötsch V. (2010) The C-terminus of p63 contains multiple regulatory elements with different functions. Cell Death Dis. 1:e5.

Suh EK, Yang A, Kettenbach A, Bamberger C, Michaelis AH, Zhu Z, Elvin JA, Bronson RT, Crum CP, McKeon F. (2006) p63 protects the female germ line during meiotic arrest. Nature 444:624–628.

Szabo A, Langer T, Schröder H, Flanagan J, Bukau B and Hartl FU. (1994) The ATP hydrolysis-dependent reaction cycle of the Escherichia coli Hsp70 system DnaK, DnaJ, and GrpE. Proc. Natl Acad. Sci. USA 91,10345–10349

Thanos CD, Goodwill KE, and Bowie JU. (1999) Oligomeric structure of the human EphB2 receptor SAM domain. Science 283: 833–836.

Thanos CD, Bowie JU. (1999) p53 Family members p63 and p73 are SAM domain-containing proteins. Protein Sci 8: 1708–1710

Thomason HA, Zhou H, Kouwenhoven EN, Dotto GP, Restivo G, Nguyen BC, Little H, Dixon MJ, van Bokhoven H, Dixon J. (2010) Cooperation between the transcription factors p63 and IRF6 is essential to prevent cleft palate in mice. J Clin Invest 120:1561-1569.

Truong AB, Kretz M, Ridky TW, Kimmel R, & Khavari PA. (2006) p63 regulates proliferation and differentiation of developmentally mature keratinocytes. Genes Dev 20(22):3185-3197.

Van Bokhoven H, Brunner HG. (2002) Splitting p63. Am J Hum Genet 71:1-13.

Van Bokhoven H, Hamel BC, Bamshad M, Sangiorgi E, Gurrieri F, Duijf PH, Vanmolkot KR, van Beusekom E, van Beersum SE, Celli J, Merkx GF, Tenconi R, Fryns JP, Verloes A, Newbury- Ecob RA, Raas-Rotschild A, Majewski F, Beemer FA, Janecke A, Chitayat D, Crisponi G, Kayserili H, Yates JR, Neri G, Brunner HG. (2001) p63 Gene mutations in eec syndrome, limb-mammary syndrome, and isolated split hand-split foot malformation suggest a genotype–phenotype correlation. Am J Hum Genet 69:481–492.

Van Bokhoven H, Melino G, Candi E, & Declercq W. (2011) p63, a story of mice and men. J Invest Dermatol 131(6):1196-1207.

Wang M and Kaufman RJ. (2016) Protein misfolding in the endoplasmic reticulum as a conduit to human disease. Nature 529, 326–335.

Yamamoto A and Simonsen A. (2011) The elimination of accumulated and aggregated proteins: a role for aggrephagy in neurodegeneration. Neurobiol. Dis. 43, 17–28.

Yamamoto K, Sato T, Matsui T, Sato M, Okada T, Yoshida H, Harada A and Mori K. (2007) Transcriptional induction of mammalian ER quality control proteins is mediated by single or combined action of ATF6a and XBP1. Dev. Cell 13, 365–376.

Yang A, Kaghad M, Caput D, McKeon F. (2002) On the shoulders of giants: p63, p73 and the rise of p53. Trends Genet 18:90-95.

Yang A, Kaghad M, Wang Y, Gillett E, Fleming MD, Dotsch V, Andrews NC, Caput D, McKeon F. (1998) p63, a p53 homolog at 3q27-29, encodes multiple products with transactivating, death-inducing, and dominant-negative activities. Mol Cell 2:305-316.

Yang A, Schweitzer R, Sun D, Kaghad M, Walker N, Bronson RT, Tabin C, Sharpe A, Caput D, Crum C, McKeon F. (1999) p63 is essential for regenerative proliferation in limb, craniofacial and epithelial development. Nature 398:714-718.

Zache N, Lambert JM, Rökaeus N, Shen J, Hainaut P, Bergman J, Wiman KG, Bykov VJ. (2008) Mutant p53 targeting by the low molecular weight compound STIMA-1. Mol Oncol. 2(1):70-80.

Zenteno JC, Berdon-Zapata V, Kofman-Alfaro S, Mutchinick OM. (2005) Isolated ectrodactyly caused by a heterozygous missense mutation in the transactivation domain of TP63. Am J Med Genet Part A 134A:74–76.